ORGANOMETALLICS

Article

pubs.acs.org/Organometallics

Pyrazole-Based PCN Pincer Complexes of Palladium(II): Mono- and Dinuclear Hydroxide Complexes and Ligand Rollover C−H Activation

Wilson D. Bailey,[†] Lapo Luconi,[‡] Andrea Rossin,[‡] Dmitry Yakhvarov,[§] Sarah E. Flowers,[†] Werner Kaminsky,[†] Richard A. Kemp,*[,∥,⊥] Giuliano Giambastiani,*[,‡,§] and Karen I. Goldberg*[,†]

[†]Department of Chemistry, University of Washington, Box 351700, Seattle, Washington 98195-1700, United States

[‡]Institute of Chemistry of Organometallic Compounds ICCOM-CNR and Consorzio INSTM, Via Madonna del Piano 10, 50019 Sesto F.no Florence, Italy

[§]Kazan Federal University, 420008 Kazan, Russian Federation

[∥]Department of Chemistry and Chemical Biology, University of New Mexico, Albuquerque, New Mexico 87131, United States

[⊥]Advanced Materials Laboratory, Sandia National Laboratories, Albuquerque, New Mexico 87106, United States

Supporting Information

ABSTRACT: Palladium complexes of the novel unsymmetrical phosphine pyrazole-containing pincer ligands PCN^H (PCN^H = 1-[3-[(di-*tert*-butylphosphino)methyl]phenyl]-1*H*-pyrazole) and PCN^{Me} (PCN^{Me} = 1-[3-[(di-*tert*-butylphosphino)methyl]phenyl]-5-methyl-1*H*-pyrazole) have been prepared and characterized through single-crystal X-ray diffraction and multinuclear ^1H, $^{13}C\{^1H\}$, and $^{31}P\{^1H\}$ NMR spectroscopy. In preparations of the monomeric hydroxide species (PCN^H)Pd(OH), an unexpected N detachment followed by C−H activation on the heterocycle 5-position took place resulting in conversion of the monoanionic {P,C$^-$,N} framework into a dianionic {P,C$^-$,C$^-$} ligand set. The dinuclear hydroxide-bridged species (PCN^H)Pd(μ-OH)Pd(PCC) was the final product obtained under ambient conditions. The "rollover" activation was followed via $^{31}P\{^1H\}$ NMR spectroscopy, and dinuclear cationic μ-OH and monomeric Pd^{II} hydroxide intermediates were identified. DFT computational analysis of the process (M06//6-31G*, THF) showed that the energy barriers for the pyrazolyl rollover and for C−H activation through a σ-bond metathesis reaction are low enough to be overcome under ambient-temperature conditions, in line with the experimental findings. In contrast to the PCN^H system, no "rollover" reactivity was observed in the PCN^{Me} system, and the terminal hydroxide complex (PCN^{Me})Pd(OH) could be readily isolated and fully characterized.

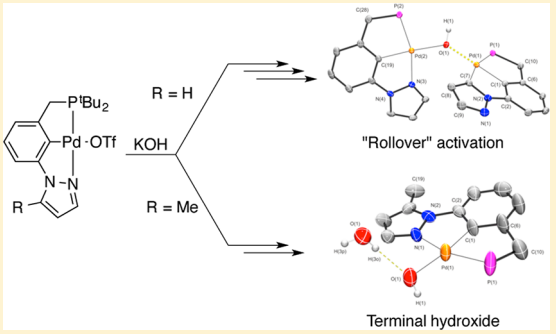

INTRODUCTION

The use of pincer-ligated transition-metal complexes as catalysts for organic transformations has grown dramatically in recent years.[1] The robust tridentate binding motif coupled with the tunability of the steric and electronic parameters of pincer ligands has proven highly effective in stabilizing and allowing isolation of a variety of uncommon types of metal complexes. For example, pincer ligands have been very useful in the preparation of mononuclear late-metal complexes bearing M−OR and M−NR_2 bonds. Notably, there are significantly fewer mononuclear late-transition-metal hydroxide, alkoxide, and amide complexes relative to their metal alkyl (M−C) analogues.[2] However, such M−OR and M−NR_2 linkages are pertinent to catalysis,[3,4] and thus isolation and study of model metal hydroxide, alkoxide and amide complexes are of great value.

The variety of available pincer ligands has increased in recent years. While early pincer ligands were symmetric with respect to ligand "arms" (e.g., PCP, PNP, POCOP, etc.),[5] pincer-type complexes bearing unsymmetrical arms have begun to appear in greater numbers (NCC, PNN, PCO, PCS, etc.).[6] PCN-type systems in particular are intriguing, because in (PCN)M(L)$_n$ complexes (M = transition metal; L = ancillary ligand) the tridentate hybrid ligand contains both *hard* (N) and *soft* (P) donor functions, thus leading to novel and unprecedented chemical properties.[7] In such species, there is a marked difference in the *trans* effect between the two different donor arms. This difference results in the group with the weaker *trans* effect (N) being more likely to dissociate from the metal center due to its position *trans* to the group with a stronger *trans* effect (P). The stronger M−P bond remains intact. From a homogeneous catalysis perspective, the hemilability of the ligand provides access to a vacant coordination site at the metal center and so can allow for effective coordination, activation, and transformation of substrate molecules. Such ligand hemilability has often been invoked as the critical factor when comparing the catalytic activity of (PCP)M(L)$_n$/

Received: April 30, 2015

DOI: 10.1021/acs.organomet.5b00355
Organometallics XXXX, XXX, XXX−XXX

(NCN)M(L)$_n$ and (PCN)M(L)$_n$ analogues; the unsymmetrical complex has consistently been shown to be *more active* than its symmetric counterparts.[6i,j,8,9]

In our laboratories, we have explored a variety of both symmetric and unsymmetrical pincer systems (PCP,[10] PNP,[11] PCO,[6h] NNC[12]) to stabilize and study model complexes. While the symmetric ligand systems result in more stable complexes, the unsymmetrical analogues have yielded higher reactivity primarily through arm lability. In a study on late-transition-metal PCO pincer systems, the ether O arm was found to be labile and allowed for reductive elimination of the pincer framework under reducing conditions.[6h] Ligand arm aromatic/heteroaromatic C−H activation through σ-bond metathesis was observed in early-transition-metal and rare-earth complexes to give unsymmetrical NNC pincer complexes.[12]

The following is an account of a novel unsymmetrical PCN pincer ligand system designed to relieve steric bulk around the metal center relative to its PCP counterpart. The nitrogen donor (pyrazolyl group) was expected to be a more strongly binding ligand than an ether linkage (as in a related PCO system) yet would potentially provide for hemilability at elevated temperatures. Notably, this is also a cautionary tale about unsymmetrical pincer ligands. Pincer ligands are often touted for their robustness, but here we find that the unsymmetrical members of the family can display unwanted reactivity of their own. The metalation of two new pyrazole-containing PCN ligand frameworks on Pd^{II} and the exploration of the reactivity of the related chloride and hydroxide complexes are discussed. In a hydroxide derivative, an unexpected pyrazolyl side arm C−H bond activation was observed. C−H addition across the Pd−OH bond on the 5-position of the heterocycle occurred to transform the monoanionic {P,C$^-$,N} ligand into a dianionic {P,C$^-$,C$^-$} donor. The thermodynamics are favorable, with the driving force for the reaction to occur provided by the simultaneous formation of a stable neutral aquo ligand that exits the metal coordination sphere. Ligand loss generates a positive entropy change and an overall (more) negative Gibbs energy variation for the side arm C−H activation reaction. The process was followed experimentally (multinuclear $^{31}P\{^1H\}$ and ^1H NMR spectroscopy) and then computationally modeled (DFT at the M06//6-31G* level of theory). By protection of the ligand in the 5-position through methylation (PCN^{Me}), this "rollover" reactivity was shut down and a stable terminal hydroxide complex was isolated.

RESULTS AND DISCUSSION

Synthesis of the PCN-Pincer Ligand PCN^H (3a). Scheme 1 summarizes the synthetic path used to obtain the PCN^H pincer ligand **3a** in fairly good yields starting from commercially available (3-bromophenyl)methanol. The phosphine group was introduced by transformation of the benzyl alcohol moiety into a better leaving group (reaction ii, bromination) followed by the phosphine nucleophilic substitution (reaction iii) as the final synthetic step. The PCN^H pincer ligand **3a** was isolated as an analytically pure and air-sensitive white solid in 48% yield from 3-bromobenzyl alcohol (see the Experimental Section).

Scheme 1. Synthesis of the Pincer PCN^H Ligand 3a[a]

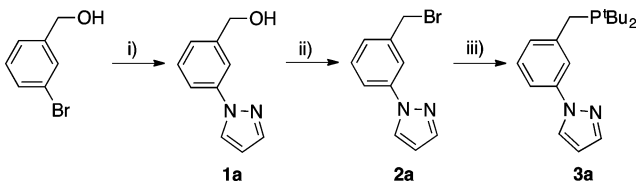

[a]Reagents and conditions: (i) pyrazole, CuI, K_2CO_3, NMP, microwave irradiation, 210 °C, 5 h, 250 W; (ii) Br_3CCO_2Et, PPh_3, CH_2Cl_2, room temperature, 0.5 h; (iii) $^tBu_2PH$, acetone, reflux, 12 h.

Synthesis of Chloro, Nitrile, and Triflate Complexes Containing the [(PCN^H)Pd]$^+$ Fragment. The reaction of PCN^H ligand **3a** with Pd(COD)Cl$_2$ in toluene (110 °C) was monitored through successive solution samplings and $^{31}P\{^1H\}$ NMR spectroscopy at room temperature. Full conversion to the Pd^{II} complex (PCN^H)PdCl (**4a**) was observed after 4 h with a new downfield $^{31}P\{^1H\}$ NMR signal at 95.1 ppm (Scheme 2).

The (PCN^H)PdCl complex **4a** was isolated as a moderately air sensitive white microcrystalline solid and was characterized by multinuclear $^{31}P\{^1H\}$, ^1H, and $^{13}C\{^1H\}$ NMR spectroscopy combined with single-crystal X-ray diffraction studies. The ^1H and $^{13}C\{^1H\}$ NMR patterns indicate that **4a** possesses C_s symmetry in solution. The most representative ^1H and $^{13}C\{^1H\}$ NMR spectroscopic resonances related to the κ^3-coordinated ligand fall at lower fields in comparison with those observed for the free ligand; the aryl carbon atom directly bound to the Pd^{II} center shows the largest resonance shift (from 120.1 (**3a**) to 150.3 (**4a**) ppm for PCN^H). Microcrystals suitable for X-ray analysis were grown from a concentrated acetone solution at −30 °C. An ORTEP representation of the crystal structure of **4a** is given in Figure 1. Table S1 (Supporting Information) gives all the main crystal and structural refinement data, and selected bond lengths and angles are summarized in Table S2 (Supporting Information).

Complex **4a** crystallizes in the orthorhombic $P2_12_12_1$ space group with four molecules per unit cell. The Pd^{II} center adopts a distorted-square-planar coordination geometry (τ_4 = 0.16).[13] Bond lengths and angles measured within the [(PCN^H)Pd]$^+$ fragment of **4a** fall in the typical range observed for related [(PCN^H)Pd]$^+$ fragments in square-planar environments.[14,9b] It is notable that the Pd−P bond in **4a** (2.227(4) Å) is shorter than those observed in symmetric (PCP)Pd(L) analogues bearing the −P^{t}Bu$_2$ group (mean Cambridge Structural Database (CSD) value 2.31 Å)[10,15] and that the Pd−N bond length in **4a** (2.094(10) Å) is longer than that found in symmetric pyrazole-based (NCN)Pd(L) species (mean CSD value 2.03 Å).[16] This crystallographic evidence suggests that the pyrazolyl group is more likely to possess hemilabile properties in the unsymmetrical PCN^H environment.

It was found that the chloride ligand *trans* to the strongly donating aryl backbone in **4a** could be abstracted by treatment of **4a** with silver reagents (Scheme 2). The nitrile complex [(PCN^H)Pd(MeCN)](BF$_4$) (**5a**) was obtained as a finely divided white powder from the reaction of **4a** with 1 equiv of AgBF$_4$ in CH_2Cl_2 in the presence of a 5-fold excess (compared to Pd) of acetonitrile. Complex **5a** was characterized by multinuclear NMR spectroscopy and elemental analysis. Unfortunately, attempts to obtain crystals of **5a** suitable for X-ray analysis were unsuccessful. The ^1H and $^{13}C\{^1H\}$ NMR resonances of **5a** are very similar to those observed for the parent chloride precursor **4a**, except for the appearance of a sharp singlet in the ^1H NMR spectrum at 2.51 ppm (ascribed to the methyl group of the coordinated CH_3CN molecule). The $^{31}P\{^1H\}$ NMR signal moves from 95.1 ppm for **4a** to 98.2 ppm for **5a**.

DOI: 10.1021/acs.organomet.5b00355
Organometallics XXXX, XXX, XXX−XXX

Scheme 2. Synthesis of the Chloride (4a, 6a), Nitrile (5a), and Triflate (7a) Pincer Complexes of PCN^H

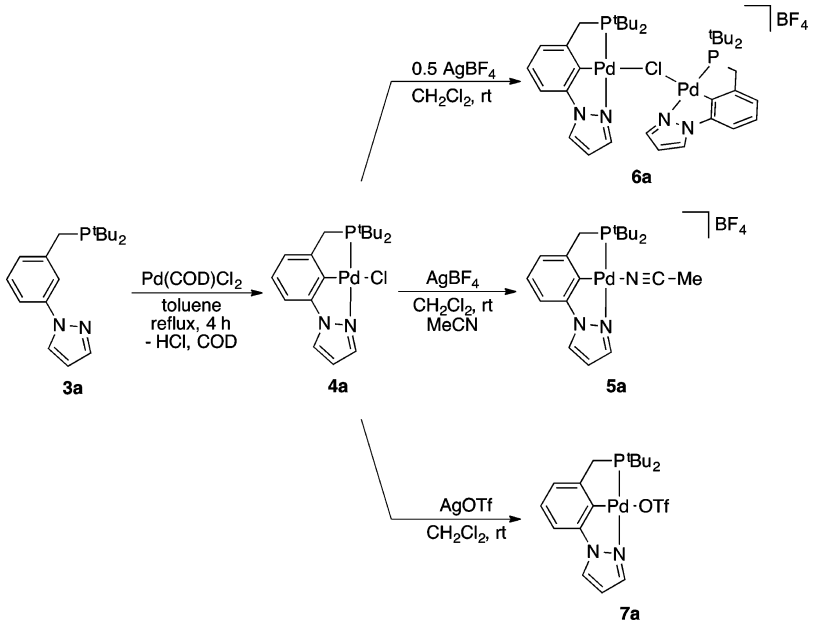

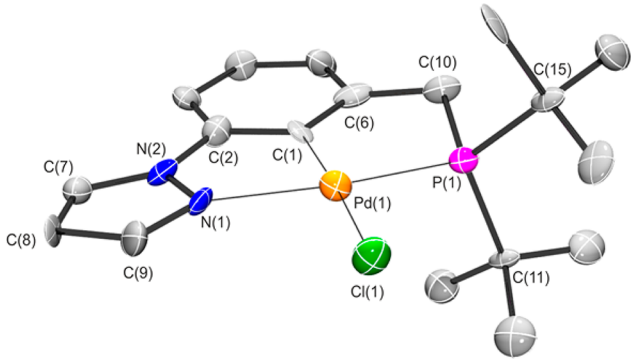

Figure 1. ORTEP representation of $(PCN^H)PdCl$ (**4a**), with ellipsoids shown at 50% probability. Hydrogen atoms are omitted for clarity.

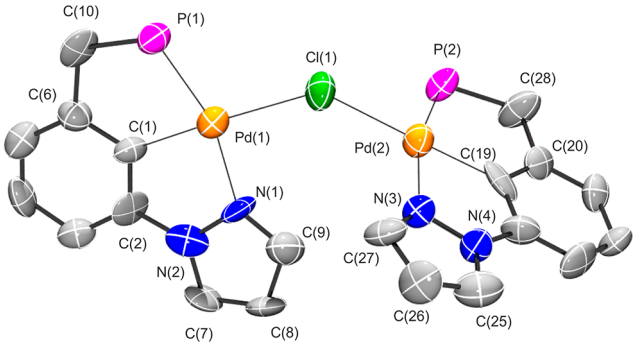

Figure 2. ORTEP representation of the cationic part of the salt $\{[(PCN^H)Pd]_2(\mu\text{-Cl})\}BF_4$ (**6a**), with ellipsoids shown at 50% probability. Hydrogen atoms, ^{t}Bu groups on P, the BF_4^- counterion, and crystallization solvent molecules are omitted for clarity.

Treatment of a CH_2Cl_2 solution of **4a** with only 0.5 equiv of $AgBF_4$ (Scheme 2) afforded the dinuclear Pd^{II} complex $\{[(PCN^H)Pd]_2(\mu\text{-Cl})\}BF_4$ (**6a**), in the form of pale yellow microcrystals. The NMR spectra of the chloride-bridged dimer show the classical patterns of C_2-symmetric species in solution, whose most representative features are given by two sharp doublets in the $^{13}C\{^1H\}$ NMR spectra: one coming from the 12 methyl groups (28.8 ppm, J_{PC} = 3.5 Hz) of the *tert*-butyl moieties and the other belonging to the ipso carbon atom σ-bound to the palladium center (149.8 ppm, J_{PC} = 13.3 Hz). As expected, a downfield sharp singlet is also observed in the $^{31}P\{^1H\}$ NMR spectrum (95.1 ppm). Microcrystals suitable for X-ray diffraction were grown by layering a concentrated CH_2Cl_2 solution of the salt with cold pentane. The solid-state structure confirmed the identity of **6a** (an ORTEP representation is given in Figure 2, and relevant bond angles and distances are given in Table S2 (Supporting Information)).

The dimer crystallizes in the orthorhombic $Pna2_1$ space group, with four molecules per unit cell. In the chloride-bridged dinuclear cation, both palladium centers maintain a slightly distorted square planar geometry. The main bond lengths and angles in **6a** are very similar to those found in the monomeric complex **4a**. Similarly to related μ-Cl monobridged cationic dimers,[17] only slightly longer Pd−Cl distances are found in **6a** (2.427(4) Å for Pd(1)−Cl(1) and 2.425(4) Å for Pd(2)−Cl(1)) in comparison to the bond length determined in **4a** (2.388(4) Å).

The reaction of **4a** with 1 equiv. of AgOTf in CH_2Cl_2 in the absence of acetonitrile yields the triflate species $(PCN^H)Pd(OTf)$ (**7a**) (Scheme 2). Complex **7a** was fully characterized by multinuclear NMR spectroscopy, X-ray crystallography, and combustion analysis. The ^1H and $^{13}C\{^1H\}$ NMR spectra display patterns very similar (albeit slightly shifted) to those observed for the chloride analogue **4a**. The $^{31}P\{^1H\}$ NMR spectrum displayed a singlet at 94.1 ppm. Complex **7a** exhibits a typical square-planar ligand arrangement about the Pd center with κ^3-PCN^H and triflate ligands coordinated. An ORTEP representation of **7a** is shown in Figure S2 (Supporting Information). Relevant bond lengths and angles appear in Table S2 (Supporting Information).

Formation of Hydroxide Species Containing the $[(PCN^H)Pd]^+$ and [(PCC)Pd] Fragments: "Rollover" C−H Bond Activation on the Pyrazolyl Side Arm. As previous transition-metal hydroxide complexes have been synthesized primarily through metathesis reactions with alkali-metal

DOI: 10.1021/acs.organomet.5b00355
Organometallics XXXX, XXX, XXX−XXX

hydroxides,[18] preparation of the desired monomeric hydroxide complex was first attempted by addition of potassium hydroxide (KOH) to the chloride complex **4a** in tetrahydrofuran (THF). No reaction was observed at room temperature, and only a slow reaction occurred to produce an array of intractable products, including palladium black, over very long reaction times (4 days) at elevated temperatures (60 °C). As group 10 terminal hydroxides have also been made via metathesis of weakly bound anions rather than from the chloride precursor,[19] the reactivity of the triflate complex **7a** with hydroxide salts was investigated.

Addition of an excess of KOH to a THF-d_8 solution of the triflate complex **7a** yielded the new product **8a**, as observed by the disappearance of the signal at 94.1 ppm and the appearance of a new singlet at 93.3 ppm in the $^{31}P\{^1H\}$ NMR spectra (Figure 3). However, further monitoring of this reaction

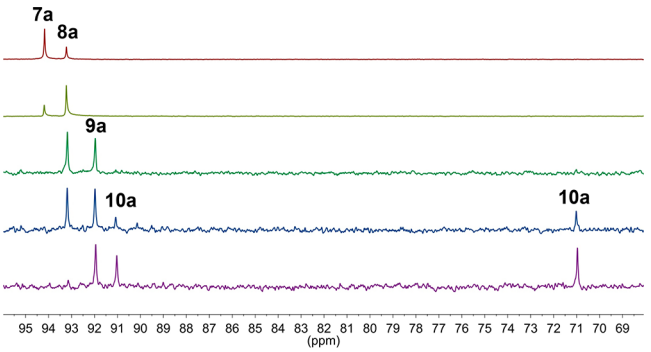

Figure 3. $^{31}P\{^1H\}$ NMR stack of the formation of species **8a**–**10a** over days.

showed conversion of **8a** to the second species **9a** with a singlet at 91.8 ppm in the $^{31}P\{^1H\}$ NMR spectrum. A third product **10a**, with two new signals at 91.1 and 71.0 ppm, then grows in concurrently with a relative decrease of the 91.8 ppm signal due to **9a**. Some decomposition of the reaction mixture was also observed in the reaction vessel as palladium black became visible. When the reaction conditions were changed as described below, characterization of the various palladium species formed in this reaction (**8a**–**10a**) was possible.

When only 0.5 equiv of KOH was added to the triflate **7a**, the new species **8a** was formed as the sole product (Scheme 3). The ^1H NMR spectrum of **8a** displays a peak at −1.48 ppm, indicative of a Pd hydroxide species. The ^{t}Bu protons appear as two doublets at 1.44 and 1.51 ppm ($^3J_{PH}$ = 14.1 and 14.3 Hz, respectively). Integration of the doublets in comparison to the hydroxide signal yields a 18:18:1 ratio, suggesting a dinuclear species. The appearance of two signals for the ^{t}Bu protons demonstrates that these positions are diastereotopic, as would be expected in a rigid nonplanar dinuclear complex. This observation is in contrast with what is found for **6a**, where only one resonance is observed for the ^{t}Bu groups at room temperature. In this case, reversible cleavage of the dinuclear complex **6a** may be occurring on the NMR time scale, resulting in the ^{t}Bu and methylene signals appearing as respectively averaged signals. Another possibility is that free rotation about the Pd–Cl bond of **6a** occurs at room temperature, although this option may be considered less likely given the similar steric profiles of **6a** and **8a**. X-ray-quality crystals of **8a** were grown from a concentrated THF solution layered with pentane. The solid-state structure confirmed the spectroscopic assignment of **8a** as the dinuclear species $\{[(PCN^H)Pd]_2(\mu\text{-OH})\}(OTf)$ (Figure 4).

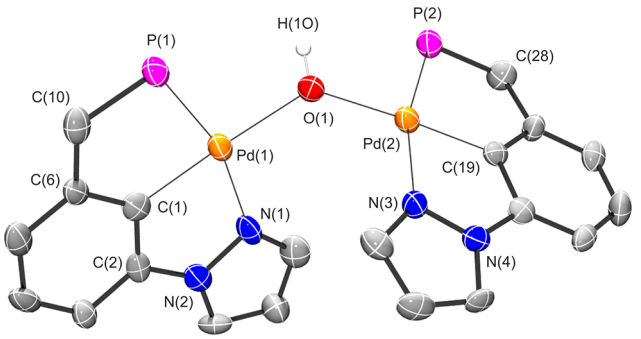

Figure 4. ORTEP representation of the cationic part of the salt $\{[(PCN^H)Pd]_2(\mu\text{-OH})\}(OTf)$ (**8a**), with ellipsoids shown at 50% probability. Hydrogen atoms, ^{t}Bu groups on P, and triflate counterion are omitted for clarity.

Dinuclear **8a** is C_2 symmetric with the two distorted-square-planar $(PCN^H)Pd$ units bridged by a single μ-OH (τ_4[Pd(1)] = 0.14; τ_4[Pd(2)] = 0.16).[13] Each palladium is formally Pd^{II}; one noncoordinating triflate counterion is found in the asymmetric unit to balance the overall positive charge of the dinuclear complex. The structure of **8a** is analogous to that of the chloride-bridged dinuclear species **6a**, with a bridging hydroxide instead of a bridging chloride. The hydroxyl hydrogen was refined by geometry optimization of the hydroxide ligand with respect to the Pd(1)–O(1) bond, while leaving the Pd(2)–O(1) bond free. The hydroxide is shielded by the bulky ^{t}Bu groups, and no hydrogen-bonding interactions were observed. The bond lengths within the $(PCN^H)Pd$ units of **8a** are similar to those observed in the mononuclear triflate complex **7a**. While bis-μ-OH dimers are well-known for Pd, this is a rare example of two palladium centers bridged only by a single μ-OH ligand.[20] Table S2 in the Supporting Information contains selected bond lengths and angles for **8a**.

When a THF solution of the triflate **7a** was treated with a full 1 equiv of KOH, **8a** was observed as a transient intermediate and decayed into complex **9a** as the major product. Complex **9a** is characterized by a singlet at 91.8 ppm in the $^{31}P\{^1H\}$ NMR spectrum. Conversion to complex **9a** was not clean, and peaks at 91.1 and 71.0 ppm (complex **10a**) in the $^{31}P\{^1H\}$ NMR

Scheme 3. Synthesis of the Hydroxide Pincer Complexes 8a–10a of the Ligand PCN^H

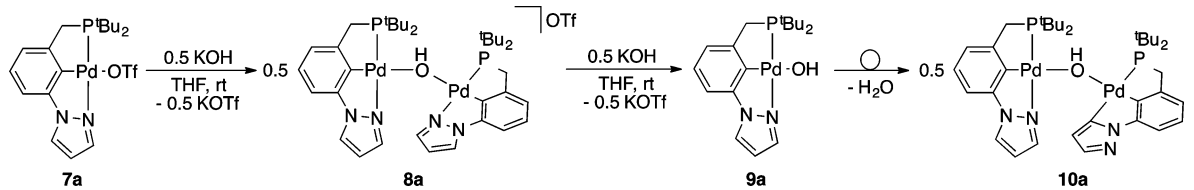

DOI: 10.1021/acs.organomet.5b00355
Organometallics XXXX, XXX, XXX–XXX

spectrum consistently appeared as a minor product, such that it was not possible to isolate pure **9a**. However, it was found that the addition of water to **9a** inhibited decomposition to **10a**. Thus, addition of D_2O to a THF-d_8 (1/4 v/v) solution of **8a** containing suspended KOH resulted in the formation of pure **9a**, which could be fully characterized in solution by NMR spectroscopy. On the basis of the intermediacy of **8a** in the formation of **9a** and the ^1H and $^{31}P\{^1H\}$ NMR spectral signals assignable to **9a**, complex **9a** is proposed to be the mononuclear terminal hydroxide $(PCN^H)Pd(OH)$ (Scheme 3). The ^1H NMR spectrum of **9a** displays a signal at −1.71 ppm (observed only in the absence of excess water), attributable to the Pd−OH group, and the ^{t}Bu protons appear as a doublet at 1.43 ppm, integrating in the ratio 18H:1H in comparison to the hydroxide signal.

Efforts to recrystallize **9a** from the reaction mixture in THF at low temperatures did yield crystals suitable for an X-ray diffraction study, as well as amorphous material. However, as shown in Figure 5, the crystallized product was not **9a** but

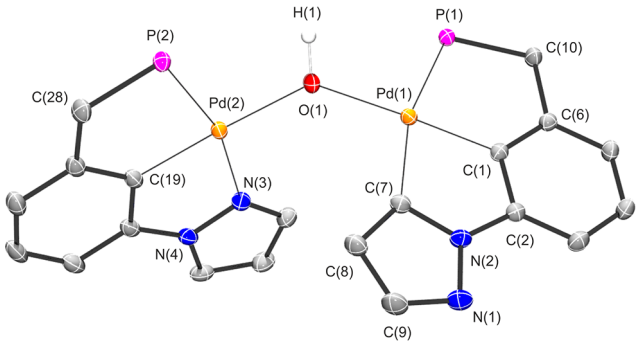

Figure 5. ORTEP representation of the $[(PCN^H)Pd](\mu\text{-}OH)[Pd(PCC)]$ dimer (**10a**), with ellipsoids shown at 50% probability. Hydrogen atoms on the pincer ligands and ^{t}Bu groups on P are omitted for clarity.

rather complex **10a**, the mixed-ligand hydroxide-bridged dinuclear complex $[(PCN^H)Pd](\mu\text{-}OH)[Pd(PCC)]$. This was confirmed, as dissolution of the isolated crystalline sample in THF yielded spectral features that matched those displayed by **10a** in the $^{31}P\{^1H\}$ NMR spectrum along with minor impurities attributed to the amorphous solid. The structure of **10a** consists of two palladium centers bridged by a single μ-OH ligand, similar to the case for **8a**. One of the Pd^{II} centers is bound by the {P,C$^-$,N} ligand as observed in **8a**. However, unlike **8a**, the other Pd^{II} center is bound to a dianionic tridentate {P,C$^-$,C$^-$} ligand; the pyrazolyl arm has "rolled over" with C−H activation having occurred at the 5-position. Details on how the pyrazolyl ring and the "rollover" ring were distinguished in the solid-state structure are presented in the Supporting Information. The $[(PCN^H)Pd]^+$ fragment displays bond angles and distances nearly identical with those found in the hydroxide complex **8a**. In contrast, the Pd(1)−P(1) bond in the [(PCC)Pd] fragment is somewhat longer than the corresponding bond in the $(PCN^H)Pd$ fragment (2.3084(4) Å vs 2.2260(4) Å). This change is expected, as the phosphorus donor is *trans* to a stronger donor when moving from neutral N to anionic C$^-$. Notably, no counterion was observed, which is consistent with the dianionic PCC character of the second pincer fragment. The Pd−O bond lengths in the cationic and neutral μ-hydroxide dimers (**8a** and **10a**, respectively) are very similar. However, when the Pd(1)−O(1) and the Pd(2)−O(1) bond lengths within **10a** are compared, a clear difference is observed. In **10a**, the hydroxide ligand is associated more with the cationic $[(PCN)Pd]^+$ fragment (2.0831(11) Å) than with the neutral [(PCC)Pd] fragment (2.1077(11) Å), further supporting a mixed-ligand dinuclear species. It should be noted that, for complex **8a**, the hydroxide ligand is shared equally between palladium centers within error.

The activation of a pyrazolyl C−H bond at the 5-position has previously been observed in (poly)pyrazolyl-containing ligands in the presence of late transition metals (e.g., Ru,[21] Pd,[22] Pt,[23] and Ir[24]), and the activation of C−H bonds by palladium fragments in several N-heterocycles has been studied computationally.[25] Notably, however, the "rollover" activation to form **10a** takes place under very mild conditions, in contrast to many previously reported literature examples that require elevated temperatures or the employment of photoirradiation. We propose that the room-temperature "rollover" C−H activation occurs at the monomeric hydroxide **9a**, forming a neutral and coordinatively unsaturated [(PCC)Pd] unit after water release (i.e., loss of an aquo ligand from the palladium coordination sphere). This is supported by the increased stability of **9a** in the presence of water (vide supra). Subsequent combination of the [(PCC)Pd] fragment with another molecule of (yet unreacted) **9a** yields the bridged species **10a** (Scheme 3). When a THF solution of a mix of **9a** as the major product and **10a** as a minor impurity was left at room temperature for 6 days, decomposition of **9a** occurred, yielding **10a** as the major product, along with unidentified side products as observed by multinuclear NMR spectroscopy. Attempts to obtain a pure sample of **10a** in solution were unsuccessful. However, by analyzing a mixture of **9a** converting to **10a** before further decomposition, signals attributed to the mixed ligand complex **10a** could be, in part, made by NMR spectroscopy. Notably, the ^1H NMR spectrum of the mixture shows four new ^{t}Bu signals (1.36, 1.39, 1.44, and 1.51 ppm), each as doublets, indicating that the substituents are not only diastereotopic as in complex **8a** but are bound to two chemically inequivalent phosphorus atoms. This is expected, as one phosphine arm is *trans* to N and the other *trans* to C. This mixed-ligand framework is also observed by four sets of doublets of doublets for the diastereotopic methylene protons (3.08, 3.12, 3.42, and 3.49 ppm), as well as four ^{t}Bu primary carbon signals in the $^{13}C\{^1H\}$ NMR spectrum (29.46, 29.51, 29.91, and 30.10 ppm; $^2J_{PC}$ = 3.9, 3.5, 6.0, and 6.0 Hz, respectively). Unfortunately, due to the complexity of the mixture and the inability to isolate **10a**, the other resonances in the $^{13}C\{^1H\}$ NMR spectrum could not be assigned confidently. To explore this "rollover" activation in more detail, DFT simulations of the reaction were undertaken.

DFT Simulation of the "Rollover" Cyclometalation in the Conversion of the Mononuclear Hydroxide 9a to the Dinuclear μ-OH Complex 10a. The pyrazolyl "rollover" and related activation of the C(5)−H pyrazolyl bond to form H_2O was examined computationally on the real system at the M06//6-31G* level of theory. THF solvent was included in the calculation through a continuum model (SMD), and all the figures reported here should be considered as ΔG or $\Delta G^{\ddagger}$ values evaluated in THF (see Computational Details). A water molecule generated by an intermolecular rearrangement of the hydroxide complex **9a** implies a $(PCN^H)^- \leftrightarrow (PCC)^{2-}$ conversion, which is proposed on the basis of the experimental results wherein the dinuclear complex $(PCN^H)Pd(\mu\text{-}OH)Pd(PCC)$ (**10a**) was isolated. The rotation of the pyrazolyl ring

DOI: 10.1021/acs.organomet.5b00355
Organometallics XXXX, XXX, XXX−XXX

around the C(2)−N(2) bond (Figure 1 for atom numbering) within the pincer can lead to an activation of the C−H bond in the 5-position by the palladium center, with concomitant formation of the *aquo* species (PCC)Pd(H_2O) (**11a**) as the result of a proton transfer to the −OH group on palladium. Beginning with the mononuclear hydroxide complex **9a**, rotation of the pyrazolyl substituent by 180° with respect to the starting geometry yields an isomeric form of the hydroxide (PCCH)Pd(OH) (**9a′**), wherein the C−H bond in the 5-position interacts with the metal center through an agostic interaction (optimized d[C−Pd] = 2.58 Å; d[H−Pd] = 2.29 Å; d[C−H] = 1.09 Å). This optimized structure is drawn in Figure 6. Unsurprisingly, N-coordination is more stabilizing than a C−H agostic interaction and the Gibbs energy of **9a′** is higher than that of **9a** by 17.0 kcal mol^{-1}.

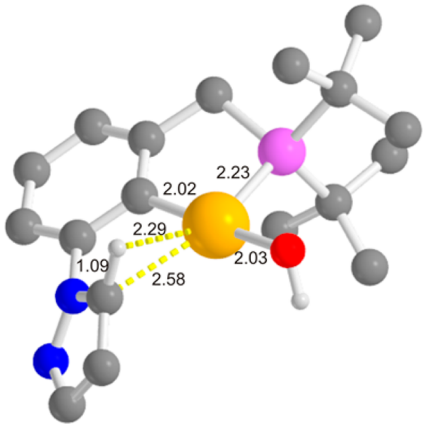

Figure 6. Optimized structure of (PCCH)Pd(OH) (**9a′**). Selected bond lengths and distances (Å) reported. H atoms on the pincer omitted for clarity. Atom color code: gray, C; white, H; red, O; blue, N; purple, P; orange, Pd.

An estimation of the rotation barrier of the pyrazolyl ring was made through a scan of the θ[C(1)−C(2)−N(2)−N(1)] dihedral angle reaction coordinate (Scheme 4 and Figure 1 for

Scheme 4. Pincer Rearrangement around the Pd Center through 180° Rotation of the Pyrazolyl Ring

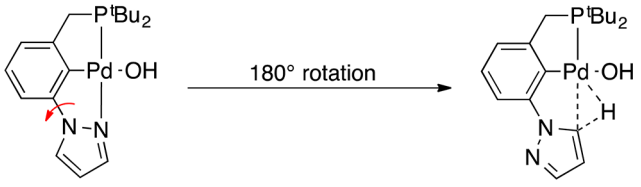

atom numbering). The maximum of the energy profile along this coordinate is located at 24.5 kcal mol^{-1} from the starting geometry (at θ(C−C−N−N) ≈ 75°), and it can be reasonably considered the "transition state" for this ligand rearrangement (Figure S54, Supporting Information).

From **9a′**, a direct proton transfer through a four-centered transition state (**TS$_1$**, Figure 7; $\Delta G^{\ddagger}$ = 20.8 kcal mol^{-1}) leads to the aquo complex **11a** (Figure 8; ΔG(**9a′**/**11a**) = −11.4 kcal mol^{-1}). The dimer formation reaction **9a** + **11a** → **10a**···**H_2O** is thermodynamically favored with ΔG = −12.0 kcal mol^{-1}. In the final structure, the water molecule engages in a hydrogen bond with the bridging hydroxide group (optimized d[μ-HO···

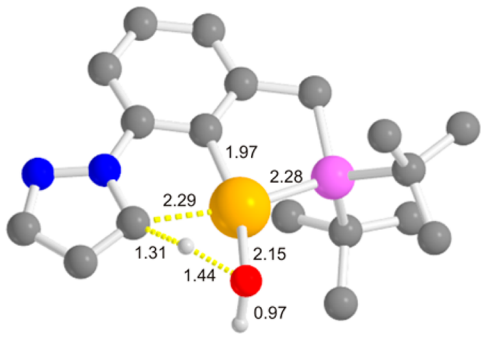

Figure 7. Optimized structure of **TS$_1$**. Selected bond lengths and distances (Å) are reported. H atoms on the pincer are omitted for clarity. For the atom color code, see the caption to Figure 6.

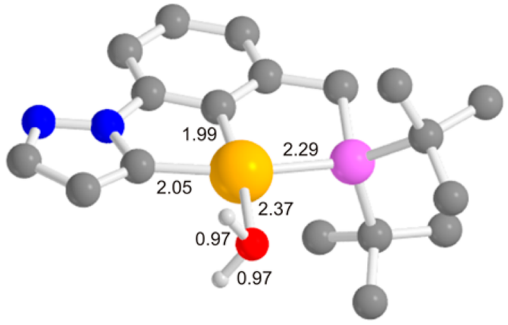

Figure 8. Optimized structure of (PCC)Pd(H_2O) (**11a**). Selected bond lengths and distances (Å) are reported. H atoms on the pincer are omitted for clarity. For the atom color code, see the caption to Figure 6.

H_2O] = 1.83 Å) and it is responsible for an extra stabilization of the dinuclear product. The optimized structure of **10a**···**H_2O** is reported in Figure 9. Evolution to the dimeric product provides

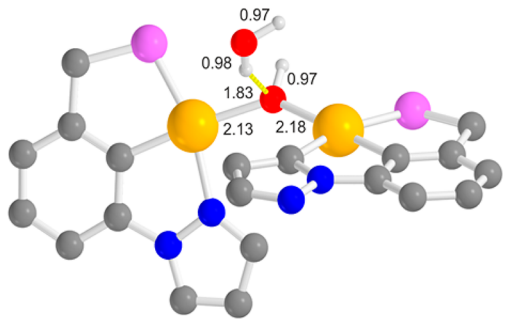

Figure 9. Optimized structure of [(PCN^H)Pd(μ-OH)Pd(PCC)]···H_2O (**10a**···H_2O). Selected bond lengths and distances (Å) are reported. H atoms on the pincer and *tert*-butyl groups on phosphorus are omitted for clarity. For the atom color code, see the caption to Figure 6.

the strong driving force for the reaction to take place. Interestingly, the pyrazolyl rotation and the C−H activation barriers are almost identical at the computational level used; thus, the heterocycle rotation (albeit slow at ambient temperature, owing to the relatively high $\Delta G^{\ddagger}$ found) is accompanied by a *simultaneous* C−H activation on the 5-position and dimer formation, as found experimentally. Notably, this analysis is consistent with experimental results, as the aquo species **11a** was never detected in the course of the

DOI: 10.1021/acs.organomet.5b00355
Organometallics XXXX, XXX, XXX−XXX

transformation of **9a** to **10a** by $^{31}P\{^{1}H\}$ NMR spectroscopy. The overall Gibbs energy vs reaction coordinate profile for this transformation is reported in Scheme 5.

Scheme 5. Gibbs Energy (THF) vs Reaction Coordinate Profile for the Formation of the Dinuclear Species 10a···H_2O Starting from the Hydroxide Complex 9a

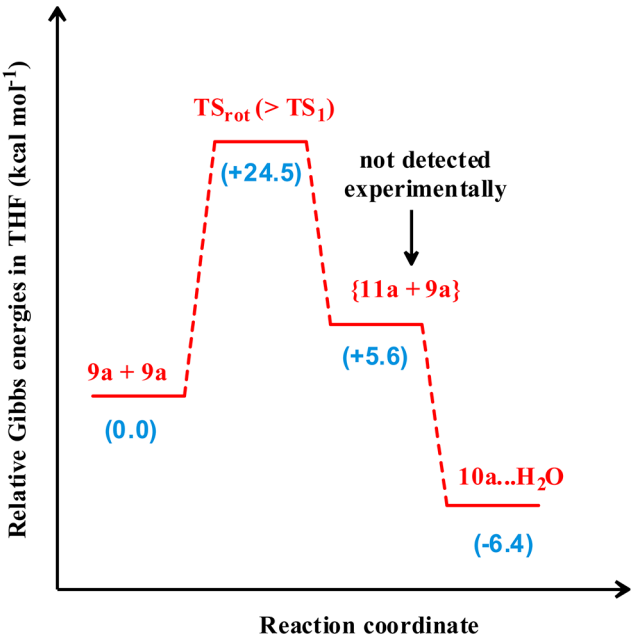

Synthesis of the Protected PCN^{Me} Ligand and the Corresponding Species of the [(PCN^{Me})Pd]$^+$ Fragment. Conversion of the mononuclear hydroxide complex **9a** to the rollover cyclometalated dinuclear **10a** should be inhibited if the 5-position of the pyrazolyl ring is blocked. With this in mind, the ligand PCN^{Me} (**3b**), which bears a methyl group at the 5-position of the pyrazolyl, was prepared (Scheme 6). The

Scheme 6. Synthesis of the Pincer PCN^{Me} Ligand 3b[a]

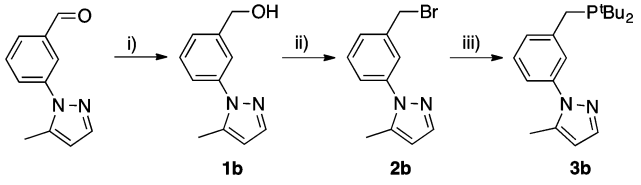

[a]Reagents and conditions: (i) $NaBH_4$, EtOH, room temperature, 1 h; (ii) Br_3CCO_2Et, PPh_3, CH_2Cl_2, room temperature, 0.5 h; (iii) $^tBu_2PH$, acetone, reflux, 12 h.

PCN^{Me} ligand **3b** was synthesized following a similar preparation from the PCN^{H} ligand **3a**, but starting from the previously reported 3-(5-methyl-1*H*-pyrazol-1-yl)-benzaldehyde.[6b] The phosphine arm was installed from the benzyl bromide derivative, which after workup gave the analytically pure off-white viscous and air-sensitive oil **3b** in 52% isolated yields from the aldehyde starting complex, as shown in Scheme 6 (see the Experimental Section).

Metalation of **3b** onto Pd^{II} to form the chloride complex (PCN^{Me})PdCl (**4b**) was carried out in a manner analogous to the metalation of **3a** (vide supra and Scheme 7). Complex **4b** was characterized by multinuclear $^{31}P\{^{1}H\}$, ^{1}H, and $^{13}C\{^{1}H\}$

Scheme 7. Synthesis of the Chloride (4b) and Triflate (7b) Pincer Complexes of PCN^{Me}

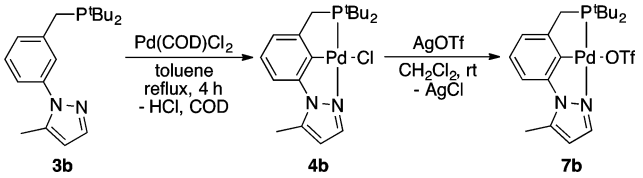

NMR spectroscopy as well as by single-crystal X-ray diffraction. Similar to its PCN^{H} analogue **4a**, complex **4b** displays C_s symmetry in solution. The spectroscopic signals for **4b** are nearly identical with those of **4a**, with the exception of the appearance of a methyl signal in the ^{1}H and $^{13}C\{^{1}H\}$ NMR spectra at 2.71 and 13.9 ppm, respectively, and a corresponding loss of the pyz-H signal at the 5-position. A singlet at 93.3 ppm is observed in the $^{31}P\{^{1}H\}$ NMR spectrum. An ORTEP representation of the solid-state structure of **4b** is presented in Figure S1 in the Supporting Information. The bond distances and angles of **4b** are very similar to those of **4a**.

When **4b** was treated with 1 equiv of silver triflate in methylene chloride at room temperature, AgCl precipitation occurred over 5 h and the Pd^{II} triflate complex (PCN^{Me})Pd-(OTf) (**7b**, Scheme 7) was formed. Complex **7b** was characterized by NMR spectroscopy, X-ray diffraction, and elemental analysis. The ^{1}H and $^{13}C\{^{1}H\}$ NMR spectra of **7b** are very similar to those of the nonmethylated analogue **7a**, differing in the appearance of a methyl resonance at 2.68 and 14.56 ppm, respectively. The $^{31}P\{^{1}H\}$ NMR spectrum of **7b** displays a singlet at 92.1 ppm. Similar to the case for **7a**, the solid-state structure of **7b** shows a square-planar complex with the triflate ligand directly bound to the Pd center (Figure S3 in the Supporting Information). The physical metrics of **7b** are closely related to those of the PCN^{H} analogue **7a**, diverging with respect to the Pd−N interaction; a shorter Pd−N distance of 2.0779(16) Å is found in **7b** in comparison to 2.112(2) Å in **7a**. Table S2 in the Supporting Information gives a selection of bond lengths and angles in the X-ray structure of **7b**.

When 0.5 equiv of KOH was added to a solution of **7b** in THF (Scheme 8), formation of the new species **8b** was

Scheme 8. Synthesis of the Hydroxide (8b, 9b) Pincer Complexes of PCN^{Me}[a]

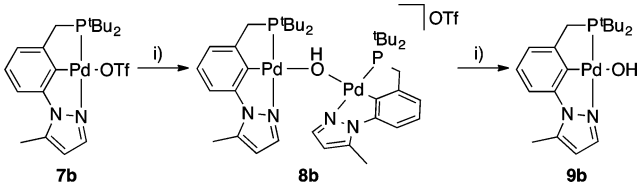

[a]Reagents and conditions: (i) 0.5 KOH, THF, room temperature.

observed by $^{31}P\{^{1}H\}$ NMR spectroscopy through the appearance of a new singlet at 91.6 ppm. This chemical shift variation (from the triflate species **7b** at 92.1 ppm) was very similar to the shift observed on going from **7a** to **8a** in the PCN^{H} system, suggesting that a similar μ-OH species had formed. Indeed, **8a** was identified as the symmetric dinuclear species {[(PCN^{Me})Pd]$_2$(μ-OH)}(OTf) by NMR spectroscopy and single-crystal X-ray diffraction. The ^{1}H NMR spectrum shows a diagnostic Pd−OH signal at −1.46 ppm, and integration of the ^{1}H NMR signals was consistent with the

DOI: 10.1021/acs.organomet.5b00355
Organometallics XXXX, XXX, XXX−XXX

presence of 2 equiv of PCN^{Me} ligand per hydroxide group. Similar to **8a**, the ^{t}Bu protons in **8b** are diastereotopic and appear as two doublets at 1.43 and 1.49 ppm ($^{3}J_{PH}$ = 14.0 and 14.2 Hz, respectively). The solid-state structure (Figure S4 in the Supporting Information) displays two nearly identical $[(PCN^{Me})Pd]^{+}$ fragments equally sharing the bridging hydroxide ligand. An outer-sphere triflate counterion is associated with the dinuclear species. While the Pd−N distance of **8b** is comparable to that of **8a**, the Pd−P bond of **8b** (2.2381(11) Å) is lengthened in comparison to **8a** (2.218(2) Å). Otherwise, the physical parameters in the solid state (bond angles and distances) between **8b** and **8a** are nearly indistinguishable.

Addition of a full 1 equiv of KOH to the bridging dinuclear hydroxide complex **8b**, or addition of an excess of KOH to the mononuclear triflate complex **7b**, cleanly yielded the new product **9b**, as observed by NMR spectroscopy (Scheme 8). A singlet at 90.2 ppm appeared with no additional signals in the $^{31}P\{^{1}H\}$ NMR spectrum. The similarity of the reaction and the chemical shift change to that found for the PCN^{H} analogue suggests that **9b** is a monomeric Pd^{II} hydroxide complex. Indeed, a new signal was observed at −1.97 ppm in the ^{1}H NMR spectrum, corresponding to a palladium hydroxide group. The upfield signal integrated to 1 equiv relative to the PCN^{Me} signals. The $^{13}C\{^{1}H\}$ NMR signals for this complex were also consistent with the assignment of **9b** as $(PCN^{Me})Pd(OH)$. While the reaction of the palladium triflate complex **7b** or the dinuclear bridging hydroxide complex **8b** with KOH produced **9b**, it was also determined that the same complex could be prepared directly from the chloride **4b**. Thus, a metathesis reaction between **4b** and an excess of KOH in THF, performed with sonication, yielded **9b** directly with no observation of a bridging species such as **8b**. As hypothesized, the mononuclear hydroxide complex **9b** was not found to undergo further reaction (i.e. "rollover" cyclometalation) as was observed for the PCN^{H} analogue **9a**. Thus, it was possible to purify complex **9b** through crystallization, and an X-ray diffraction study was used to confirm the solid-state structure (Figure 10).

Complex **9b** crystallizes in the orthorhombic $P2_12_12$ space group, with two monomers, two water molecules, and three disordered THF solvent molecules per asymmetric unit. The square-planar Pd^{II} center is bound by the tridentate PCN^{Me} ligand with a hydroxide ligand occupying the fourth coordination site. Each complex is hydrogen-bound to a symmetry-related copy of itself via two water molecules and the hydroxyl ligand. This water-bridged mode has been observed previously in terminal hydroxides.[19,26] The $[(PCN^{Me})Pd]^{+}$ fragment has metrics (bond angles and distances) similar to those of the other monomeric $(PCN^{H,Me})PdX$ (X = Cl, OTf) structures described above.

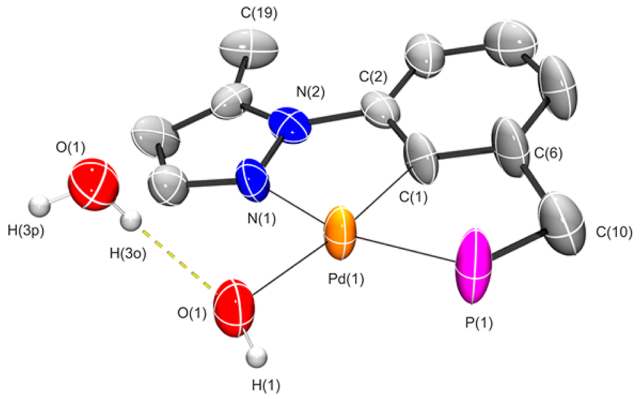

Figure 10. ORTEP representation of the $(PCN^{Me})Pd(OH)$ complex **9b**, with ellipsoids shown at 50% probability. Hydrogen atoms and ^{t}Bu groups on the pincer ligands are omitted for clarity. The Pd−HO···H_2O hydrogen bond between the hydroxyl group and the crystallization water molecule is depicted by a yellow dotted line.

The Pd−O bond length (2.078(7) and 2.080(7) Å from two molecules in the asymmetric unit) is comparable to that found in the handful of other monomeric Pd^{II}−OH complexes that have been characterized in the solid state (mean CSD value 2.05 Å).[27] For example, the Pd^{II}−OH bond length reported for the pincer complex $(^{tBu}PCP)Pd(OH)\cdots H_2O$ was 2.095 Å.[28]

CONCLUSIONS

We have reported the synthesis and characterization of a new unsymmetrical pincer ligand scaffold and complexation of these novel PCN ligands to Pd^{II}. With a bulky phosphine and a less sterically hindered pyrazolyl as the arms on the PCN pincer ligand, both mononuclear and dinuclear Pd^{II} hydroxide complexes were formed and characterized. Furthermore, a pyrazolyl ring "rollover" activation at the metal center was observed on a pyrazolyl pincer complex bearing an available C−H bond at the 5-position of the pyrazolyl side arm. Observation of this reactivity provides opportunities for the synthesis of new derivatives of the dianionic tridentate $(PCC)^{2-}$ fragment, and it also serves as a warning to those interested in exploiting the "stability" of PCN-ligated structures. Notably, the use of the methylated analogue (PCN^{Me}) inhibits the "rollover" reactivity, allowing for a clean isolation of the mononuclear hydroxide species. Studies to explore the reactivity of the novel mono- and dinuclear hydroxide complexes with small molecules of interest in renewable energy (H_2) or carbon capture and sequestration (CO_2) research are planned.

EXPERIMENTAL SECTION

General Considerations and Materials Characterization. All air- and/or moisture-sensitive reactions were performed under an inert atmosphere in flame-dried flasks using standard Schlenk-type techniques or in a glovebox filled with nitrogen. Tetrahydrofuran (THF) was purified by distillation from sodium/benzophenone ketyl, after drying over KOH or used after passage through columns of activated alumina and molecular sieves. Benzene, *n*-hexane, pentane, CH_3CN, and toluene were purified by distillation from sodium/triglyme benzophenone ketyl or were obtained by means of a MBraun solvent purification system. Pentane and CH_2Cl_2 were also used after passage through columns of activated alumina and molecular sieves. THF-d_8, benzene-d_6, and toluene-d_8 were dried over sodium/benzophenone ketyl, condensed in vacuo over activated 4 Å molecular sieves, and degassed by several freeze−pump−thaw cycles prior to use. CD_2Cl_2 was dried over activated 4 Å molecular sieves or calcium hydride. All other reagents and solvents were used as purchased from commercial suppliers. ^{1}H, $^{13}C\{^{1}H\}$, and $^{31}P\{^{1}H\}$ NMR spectra were obtained on a Bruker Avance 700, Bruker Avance 500, Bruker Avance DRX-400, or Bruker Avance 300 MHz instrument. Chemical shifts are reported in ppm (δ) relative to TMS, referenced to the chemical shifts of residual solvent resonances (^{1}H and ^{13}C), and coupling constants are given in Hz. $^{31}P\{^{1}H\}$ NMR spectra are referenced to an external 85% H_3PO_4 sample (0 ppm). The N, C, H elemental analyses were carried out at ICCOM by means of a Carlo Erba Model 1106 elemental analyzer or at the CENTC Elemental Analysis Facility at the University of Rochester. The GC/MS analyses were performed on a Shimadzu QP2010S apparatus equipped with a column identical with that used for GC analysis.

DOI: 10.1021/acs.organomet.5b00355
Organometallics XXXX, XXX, XXX−XXX

X-ray Diffraction Data. X-ray diffraction intensity data were collected on an Oxford Diffraction XcaliburPX (**4a**,**b** and **6a**) equipped with a CCD area detector or on a Bruker APEX II (**7a**,**b**, **8a**,**b**, **9b**, and **10a**) diffractometer using Mo Kα radiation (λ = 0.71073 Å) at low temperature (either T = 100 or 120 K, see Table S1 in the Supporting Information). The data set was integrated and scaled using SAINT and SADABS within the APEX2 software package by Bruker.[29] The program used for the data collection was CrysAlis CCD 1.171.[30] Data reduction was carried out with the program CrysAlis RED 1.171,[31] and the absorption correction was applied with the program ABSPACK 1.17. Direct methods implemented in Sir97[32] were used to solve the structures, and the refinements were performed by full-matrix least squares against F^2 implemented in SHELX97.[33] All of the non-hydrogen atoms were found from Fourier syntheses of electron density and were refined anisotropically, while the hydrogen atoms were fixed in calculated positions and refined isotropically with the thermal factor depending on the atom to which they are bound (riding model), with C···H distances in the range 0.95−1.00 Å. The geometrical calculations were performed by PARST97.[34] The details of crystallographic, collection, and refinement data are shown in Table S1. Molecular plots were produced by the program ORTEP3.[35]

CCDC 1048866 (**4a**), 1048867 (**4b**), 1048868 (**6a**), 1061228 (**7a**), 1061229 (**7b**), 1061230 (**8a**), 1061231 (**8b**), 1061232 (**9b**), and 1061233 (**10a**) contain supplementary crystallographic data for this paper. These data can be obtained free of charge from The Cambridge Crystallographic Data Centre via ccdc.cam.ac.uk/community/requestastructure.

Computational Details. Density functional theory (DFT) calculations were performed using the Gaussian09 program (revision C.01).[36] Model structures were optimized with a M06 functional[37] using the SDD/MWB10 pseudopotential and related basis set[38] on the palladium and phosphorus atoms plus a 6-31G* basis set on all the other atoms. Introduction of diffuse functions is essential to well reproduce conformational equilibria and experimental electron affinities.[39] An extra d-type polarization function for P and an extra f-type function for Pd were added to the standard set.[40] Gibbs energy calculations to infer relative thermodynamic stabilities were carried out on the real system. The initial guess geometry for the optimization was obtained by starting from the XRD structure of the dimeric species **10a**. IRC analysis[41] was performed to find the two minima linked by the related transition structure. When IRC calculations failed to reach the minima, geometry optimizations from the initial phase of the IRC path were performed. Frequency calculations were made on all the optimized structures, to characterize the stationary points as minima or TSs and calculate zero-point energies, enthalpies, entropies, and gas-phase Gibbs energies at 298 K. Evaluation of the solvent effects was performed through a continuum modeling of the reaction medium. Bulk solvent effects (THF, θ = 7.42) were expressed through the SMD Continuum Model,[42] with the same basis set used for the gas phase optimizations. The Gibbs energy in solution was calculated according to the following simplified equation: $G_{THF} = G_{gas} + (E_{THF} - E_{gas})$.

Synthesis of (3-(1*H*-Pyrazol-1-yl)phenyl)methanol (1a). To a solution of (3-bromophenyl)methanol (1.00 g, 5.34 mmol) in *N*-methylpyrrolidinone (NMP, 32 mL) were added K_2CO_3 (1.47 g, 10.68 mmol), CuI (0.10 g, 0.53 mmol), and pyrazole (0.38 g, 5.61 mmol) in sequence. The reaction mixture was placed in a microwave apparatus (CEM Discover) and heated at 210 °C for 5 h while a constant irradiation power was maintained (250 W). The mixture was then cooled to room temperature and filtered on a Celite pad to remove all suspended residues, and AcOEt (50 mL) was used to wash the filter. The collected organic phase was evaporated in vacuo to give a viscous residue that was purified by flash chromatography (silica gel, petroleum ether/AcOEt 60/40) to give **1a** as a pale yellow oil (0.73 g, yield 78.6%). ^{1}H NMR (300 MHz, $CDCl_3$, 293 K): δ 3.80 (br s, 1H, CH_2OH), 4.64 (s, 2H, CH_2OH), 6.42 (m, 1H, C*H*), 7.18 (m, 1H, C*H* Ar), 7.32 (m, 1H, C*H* Ar), 7.50 (m, 1H, C*H* Ar), 7.60 (br s, 1H, C*H* Ar), 7.66 (m, 1H, C*H*), 7.85, (m, 1H, C*H*). ^{13}C{^{1}H} NMR (75 MHz, $CDCl_3$, 293 K): δ 64.2 (s), 107.6 (s), 117.6 (s), 118.1 (s), 124.8 (s), 127.1 (s), 129.4 (s), 140.0 (s), 140.9 (s), 142.9 (s). Anal. Calcd for $C_{10}H_{10}N_2O$ (174.20): C, 68.95; H, 5.79; N, 16.08. Found: C, 69.05; H, 5.84; N, 16.17.

Synthesis of (3-(5-Methyl-1*H*-pyrazol-1-yl)phenyl)methanol (1b). To a stirred solution of 3-(5-methyl-1*H*-pyrazol-1-yl)-benzaldehyde (0.415 g, 2.22 mmol) in dry and degassed EtOH (10 mL) was added $NaBH_4$ (0.126 g, 3.34 mmol) in one portion. The reaction mixture was stirred at room temperature for 1 h before being quenched with water (10 mL). The mixture was then extracted with AcOEt (3 × 20 mL), and the combined organic layers were dried over Na_2SO_4. Filtration and solvent removal under reduced pressure gave the crude material, which was purified by flash chromatography (silica gel; petroleum ether/AcOEt 60/40) to give **1b** as an off-white oil (0.367 g, yield 87.8%). ^{1}H NMR (300 MHz, CD_2Cl_2, 293 K): δ 2.31 (s, 3H, CH_3), 2.94 (br s, 1H, CH_2OH), 4.65 (s, 2H, CH_2OH), 6.19 (m, 1H, C*H*), 7.33−7.28 (2H, C*H* Ar), 7.44−7.37 (2H, C*H* Ar), 7.51 (m, 1H, C*H* Ar). ^{13}C{^{1}H} NMR (75 MHz, CD_2Cl_2, 293 K): δ 12.1 (s), 64.0 (s), 106.7 (s), 123.0 (s), 123.4 (s), 125.6 (s), 128.8 (s), 138.9 (s), 139.6 (s), 139.9 (s), 142.9 (s). Anal. Calcd for $C_{11}H_{12}N_2O$ (188.23): C, 70.19; H, 6.43, N, 14.88. Found: C, 70.39; H, 6.65; N, 14.93.

General Procedure for Bromination of the Benzyl Alcohol Intermediates 1a,b: Synthesis of 1-(3-(Bromomethyl)phenyl)-1*H*-pyrazole (2a) and 1-(3-(Bromomethyl)phenyl)-5-methyl-1*H*-pyrazole (2b). To a stirred solution of the selected alcohol (**1a** or **1b**) intermediate (5 mmol) and PPh_3 (1.97 g, 7.5 mmol) in dry and degassed CH_2Cl_2 (30 mL) was added Br_3CCO_2Et (0.93 mL, 5 mmol) dropwise under an N_2 atmosphere. After 30 min of stirring at room temperature, the reaction mixture was quenched with water and the formed layers were separated. The aqueous phase was washed with CH_2Cl_2 (3 × 15 mL), and the combined organic extracts were dried over Na_2SO_4. After solvent removal the resulting semisolid material was washed with hot hexane (3 × 15 mL) and the organic phases were separated from PPh_3 (and $OPPh_3$) residues upon filtration. The crude residue was then purified by flash chromatography (silica gel; petroleum ether/AcOEt 80/20) to give **2a**,**b** as off-white viscous oils in 68.5% and 67.7% isolated yields, respectively.

*Compound **2a**.* ^{1}H NMR (300 MHz, $CDCl_3$, 293 K): δ 4.52 (s, 2H, CH_2Br), 6.47 (m, 1H, C*H*), 7.30 (m, 1H, C*H* Ar), 7.42 (t, 1H, $^3J_{HH}$ = 7.8 Hz, C*H* Ar), 7.60 (m, 1H, C*H* Ar), 7.73 (m, 1H, C*H*), 7.77 (br s, 1H, C*H* Ar), 7.93, (m, 1H, C*H*). ^{13}C{^{1}H} NMR (75 MHz, $CDCl_3$, 293 K): δ 32.6 (s), 107.8 (s), 118.9 (s), 119.8 (s), 126.7 (s), 126.9 (s), 129.9 (s), 139.3 (s), 140.0 (s), 141.2 (s). Anal. Calcd for $C_{10}H_9BrN_2$ (237.10): C, 50.66; H, 3.83; N, 11.82. Found: C, 50.78; H, 3.89; N, 11.90.

*Compound **2b**.* ^{1}H NMR (300 MHz, CD_2Cl_2, 293 K): δ 2.36 (s, 3H, CH_3), 4.56 (s, 2H, CH_2Br), 6.21 (m, 1H, C*H*), 7.48−7.37 (3H, C*H* Ar), 7.54−7.52 (2H, C*H* Ar). ^{13}C{^{1}H} NMR (75 MHz, CD_2Cl_2, 293 K): δ 12.3 (s), 32.7 (s), 107.1 (s), 124.2 (s), 125.2 (s), 127.8 (s), 129.3 (s), 138.7 (s), 139.1 (s), 139.8 (s), 140.4 (s). Anal. Calcd for $C_{11}H_{11}BrN_2$ (251.12): C, 52.61; H, 4.42; N, 11.16. Found: C, 52.73; H, 4.56; N, 11.22.

General Procedure for Phosphination of the Bromine Intermediates 2a,b: Synthesis of 1-(3-((Di-*tert*-butylphosphino)methyl)phenyl)-1*H*-pyrazole (3a) and 1-(3-((Di-*tert*-butylphosphino)methyl)phenyl)-5-methyl-1*H*-pyrazole (3b). To a solution of ^{t}Bu$_2$PH (2.5 mmol) in dry and degassed acetone (10 mL) was added an acetone solution (15 mL) of the the selected bromine (**2a** or **2b**) derivative (2 mmol) in one portion. The resulting mixture was refluxed under an N_2 atmosphere for 12 h. Afterward, the cooled solution was treated with 25 mL of dry and degassed pentane, causing the precipitation of the HBr phosphine adduct (**3a**·HBr or **3b**·HBr). The collected white solid was washed with degassed pentane (3 × 15 mL) before being dissolved in 15 mL of degassed H_2O and treated with 12 mL of a degassed saturated NaOAc solution. The aqueous phase was then extracted with dry and degassed Et_2O (3 × 20 mL), and the collected (colorless) organic phases were dried over Na_2SO_4. Solvent removal gave **3a**,**b** in the form of an analytically pure white solid (for **3a**) and off-white viscous oil (for **3b**) in 88.4% and 86.8% isolated yields, respectively.

*Compound **3a**.* ^{31}P{^{1}H} NMR (121 MHz, CD_2Cl_2, 293 K): δ 35.2 (s). ^{1}H NMR (300 MHz, CD_2Cl_2, 293 K): δ 1.18 (d, $^3J_{PH}$ = 10.8 Hz,

DOI: 10.1021/acs.organomet.5b00355
Organometallics XXXX, XXX, XXX−XXX

18H, P-C(CH_3)$_3$), 2.94 (d, $^2J_{PH}$ = 2.8 Hz, 2H, Ar-−CH_2-P), 6.48 (m, 1H, C*H*), 7.38−7.30 (2H, C*H* Ar), 7.48 (m, 1H, C*H* Ar), 7.69 (m, 1H, C*H*), 7.75 (m, 1H, C*H* Ar), 7.98, (m, 1H, C*H*). $^{13}C\{^1H\}$ NMR (75 MHz, CD_2Cl_2, 293 K): δ 28.5 (d, J_{PC} = 24.7 Hz, Ar-CH_2-P), 29.5 (d, J_{PC} = 13.2 Hz, P-C(CH_3)$_3$), 31.6 (d, $^1J_{PC}$ = 22.7 Hz, P-$C(CH_3)_3$), 107.2 (s), 115.8 (s), 120.1 (d, J_{PC} = 9.3 Hz), 126.6 (s), 127.6 (d, J_{PC} = 8.5 Hz), 129.0 (s), 140.0 (s), 140.7 (s), 143.8 (d, J_{PC} = 13.0 Hz). Anal. Calcd for $C_{18}H_{27}N_2P$ (302.39): C, 71.49; H, 9.00, N, 9.26. Found: C, 71.60; H, 9.21, N, 9.30.

Compound **3b**. $^{31}P\{^1H\}$ NMR (121 MHz, CD_2Cl_2, 293 K): δ 35.7 (s). ^1H NMR (300 MHz, CD_2Cl_2, 293 K): δ 1.16 (d, $^3J_{PH}$ = 10.8 Hz, 18H, P-C(CH_3)$_3$), 2.34 (s, 3H, CH_3), 2.92 (d, $^2J_{PH}$ = 2.8 Hz, 2H, Ar-CH_2-P), 6.20 (m, 1H, C*H*), 7.24−7.20 (m, 1H, C*H* Ar), 7.38−7.34 (2H, C*H* Ar), 7.45 (br s, 1H, C*H* Ar), 7.53 (m, 1H, C*H*). $^{13}C\{^1H\}$ NMR (75 MHz, CD_2Cl_2, 293 K): δ 12.2 (s), 28.3 (d, J_{PC} = 24.7 Hz, Ar-CH_2-P), 29.4 (d, J_{PC} = 13.2 Hz, P-C(CH_3)$_3$), 31.7 (d, $^1J_{PC}$ = 22.7 Hz, P-C(CH_3)$_3$), 106.5 (s), 121.6 (s), 125.8 (d, J_{PC} = 9.2 Hz), 128.6 (s), 128.7 (d, J_{PC} = 8.4 Hz), 138.7 (s), 139.4 (s), 143.4 (d, J_{PC} = 12.7 Hz). Anal. Calcd for $C_{19}H_{29}N_2P$ (316.42): C, 72.12; H, 9.24; N, 8.85. Found: C, 72.33; H, 9.40; N, 8.92.

General Procedure for the Synthesis of the Chloride Complexes 4a,b. To a stirred solution of the selected PCN^R ligand (R = H, **3a**; R = Me, **3b**) (0.5 mmol) in dry and degassed toluene (3 mL) was added a suspension of Pd(COD)Cl_2 (0.50 mmol) in dry and degassed toluene (4 mL) in one portion. The reaction mixture was stirred at reflux of solvent for 4 h, and then it was cooled to room temperature. Afterward, the solvent was removed under vacuum to give a crude mixture as a yellow pale semisolid material. The crude sample was washed with pentane and filtered to afford analytically pure white crystals of **4a,b** in 90% and 93% isolated yields, respectively. For both palladium compounds, crystals suitable for X-ray diffraction analysis were growth from concentrated acetone solutions.

(PCN^H)PdCl ***(4a)***. $^{31}P\{^1H\}$ NMR (161 MHz, CD_2Cl_2, 293 K): δ 95.0 (s). ^1H NMR (400 MHz, CD_2Cl_2, 293 K): δ 1.48 (d, $^3J_{PH}$ = 14.3 Hz, 18H, P-C(CH_3)$_3$), 3.41 (d, $^2J_{PH}$ = 9.3 Hz, 2H, Ar-CH_2-P), 6.55 (m, 1H, C*H*), 7.06−7.15 (3H, C*H* Ar), 7.98−8.02 (2H, C*H* Ar). $^{13}C\{^1H\}$ NMR (100 MHz, CD_2Cl_2, 293 K): δ 29.2 (d, $^2J_{PC}$ = 4.3 Hz, P-C(CH_3)$_3$), 35.3 (d, $^1J_{PC}$ = 31.6 Hz, Ar-CH_2-P), 35.6 (d, $^1J_{PC}$ = 19.7 Hz, P-$C(CH_3)_3$), 107.1 (s), 110.1 (s), 122.5 (d, $^3J_{PC}$ = 20.4 Hz), 125.7 (s), 126.0 (s), 139.3 (s), 143.7 (s), 148.6 (s), 150.3 (d, $^3J_{PC}$ = 14.0 Hz). Anal. Calcd for $C_{18}H_{26}ClN_2PPd$ (443.26): C, 48.77; H, 5.91; N, 6.32. Found: C, 48.82; H, 5.97; N, 6.39.

(PCN^{Me})PdCl ***(4b)***. $^{31}P\{^1H\}$ NMR (161 MHz, CD_2Cl_2, 293 K): δ 93.3 (s). ^1H NMR (400 MHz, CD_2Cl_2, 293 K): δ 1.48 (d, $^3J_{PH}$ = 14.2 Hz, 18H, P-C(CH_3)$_3$), 2.71 (s, 3H, CH_3), 3.39 (d, $^2J_{PH}$ = 9.4 Hz, 2H, Ar-CH_2-P), 6.29 (m, 1H, C*H*), 7.06 (m,1H, C*H*), 7.13 (m,1H, C*H*), 7.23 (m, 1H, C*H* Ar), 7.91 (m, 1H, C*H* Ar). $^{13}C\{^1H\}$ NMR (100 MHz, CD_2Cl_2, 293 K): δ 13.9 (s, CH_3), 28.8 (d, $^2J_{PC}$ = 4.3 Hz, P-C(CH_3)$_3$), 34.9 (d, $^1J_{PC}$ = 28.7 Hz, Ar-CH_2-P), 35.0 (d, $^1J_{PC}$ = 17.4 Hz, P-$C(CH_3)_3$), 108.0 (s), 111.3 (s), 121.6 (d, $^3J_{PC}$ = 20.4 Hz), 125.0 (s), 138.4 (s), 140.1 (s), 144.9 (s), 149.0 (s), 150.1 (d, $^3J_{PC}$ = 14.4 Hz). Anal. Calcd for $C_{19}H_{28}ClN_2PPd$ (457.29): C, 49.90; H, 6.17; N, 6.13. Found: C, 49.93; H, 6.21; N, 6.15.

[(PCN^H)Pd(MeCN)](BF_4) (5a). To a stirred solution of **4a** (0.100 g, 0.23 mmol) in dry and degassed CH_2Cl_2 (5 mL) were added dry and degassed CH_3CN (23 μL, 0.44 mmol) and $AgBF_4$ (0.065 g, 0.33 mmol) in sequence, under a nitrogen atmosphere. The resulting mixture was stirred at room temperature for 5 h, and then the solution was filtered via cannula and concentrated to approximately three-fourths of its initial volume. To this concentrated solution was added, drop by drop, dry and degassed pentane until a precipitate formed. The final white solid was washed with several portions of pentane and dried under vacuum for 1 h (0.090 g, 75% isolated yield). $^{31}P\{^1H\}$ NMR (161 MHz, CD_2Cl_2, 293 K): δ 98.2 (s). ^1H NMR (400 MHz, CD_2Cl_2, 293 K): δ 1.41 (d, $^3J_{PH}$ = 14.7 Hz, 18H, P-C(CH_3)$_3$), 2.51 (s, 1H, CH_3CN), 3.43 (d, $^2J_{PH}$ = 9.6 Hz, 2H, Ar-CH_2-P), 6.64 (m, 1H, C*H*), 7.07 (m, 1H, C*H* Ar), 7.13 (m, 1H, C*H* Ar), 7.20 (m, 1H, C*H* Ar), 7.90 (m, 1H, C*H* Ar), 8.07 (m, 1H, C*H* Ar). $^{13}C\{^1H\}$ NMR (100 MHz, CD_2Cl_2, 293 K): δ 2.9 (s, CH_3CN), 28.6 (d, J_{PC} = 4.2 Hz, P-C(CH_3)$_3$), 33.7 (d, J_{PC} = 31.2 Hz, Ar-CH_2-P), 35.5 (d, J_{PC} = 17.7 Hz, P-$C(CH_3)_3$), 107.8 (s), 110.6 (s), 122.7 (d, J_{PC} = 21.0 Hz), 126.8 (s), 126.9 (s), 140.5 (s), 143.3 (s), 143.4 (s), 150.4 (d, J_{PC} = 13.5 Hz). $^{11}B\{^1H\}$ NMR (128 MHz, CD_2Cl_2, 293 K): δ −1.0. Anal. Calcd for $C_{20}H_{29}BF_4N_3PPd$ (535.66): C, 44.84; H, 5.46; N, 7.84. Found: C, 44.88; H, 5.50; N, 7.80.

{[(PCN^H)Pd]$_2$(μ-Cl)}(BF_4) (6a). To a stirred solution of **4a** (0.100 g, 0.23 mmol) in dry and degassed CH_2Cl_2 (10 mL) was added 0.5 equiv of $AgBF_4$ (0.022 g, 0.11 mmol) under a nitrogen atmosphere. The resulting mixture was stirred at room temperature for 5 h, and then the solution was filtered via cannula and concentrated to approximately one-third of its initial volume. To this concentrated solution was added, drop by drop, dry and degassed pentane until a precipitate formed. The final pale yellow solid was washed with several portions of pentane and dried under vacuum for 1 h (0.062 g, 60% isolated yield). Crystals suitable for X-ray diffraction were obtained from a concentrated solution of the complex in a mixture of CH_2Cl_2/pentane cooled at −30 °C. $^{31}P\{^1H\}$ NMR (121 MHz, CD_2Cl_2, 293 K): δ 95.1 (s). ^1H NMR (300 MHz, CD_2Cl_2, 293 K): δ 2.17 (d, $^3J_{PH}$ = 14.4 Hz, 36H, P-C(CH_3)$_3$), 3.44 (d, $^2J_{PH}$ = 8.7 Hz, 2H, Ar-CH_2-P, H), 6.39 (m, 2H, C*H*), 7.11−7.16 (6H, C*H* Ar), 8.03−8.09 (4H, C*H* Ar). $^{13}C\{^1H\}$ NMR (75 MHz, CD_2Cl_2, 293 K): δ 28.8 (d, J_{PC} = 3.5 Hz, P-C(CH_3)$_3$), 34.0 (d, J_{PC} = 30.3 Hz, Ar-CH_2-P), 35.6 (d, J_{PC} = 17.5 Hz, P-$C(CH_3)_3$), 107.2 (s), 110.6 (s), 122.8 (d, J_{PC} = 20.5 Hz), 126.6 (s), 139.8 (s), 142.9 (s), 144.6 (s), 149.8 (d, J_{PC} = 13.3 Hz). $^{11}B\{^1H\}$ NMR (96 MHz, CD_2Cl_2, 293 K): δ −1.1. Anal. Calcd for $C_{36}H_{52}BClF_4N_4P_2Pd_2$ (937.87): C, 46.10; H, 5.59; N, 5.97. Found: C, 46.20; H, 5.63; N, 5.93.

(PCN^H)Pd(OTf) (7a). AgOTf (33.0 mg, 0.128 mmol) was added to a solution of **4a** (51.2 mg, 0.116 mmol) in CH_2Cl_2 (2 mL) in the absence of light. The suspension was stirred for 4 h and filtered through Celite. Solvent removal yielded **7a** as an off-white solid (62.7 mg, 97% yield). Recrystallization from layering pentane on a concentrated solution of **7a** in CH_2Cl_2 yielded clear crystals that were suitable for X-ray crystallography. $^{31}P\{^1H\}$ NMR (202 MHz, CD_2Cl_2): δ 94.1 (s). ^1H NMR (500 MHz, CD_2Cl_2): δ 1.43 (d, $^3J_{PH}$ = 14.5 Hz, 18H, P-C(CH_3)$_3$), 3.31 (d, $^2J_{PH}$ = 9.6 Hz, 2H, Ar-CH_2-P), 6.55 (m, 1H, C*H*), 7.01 (dd, J_{HH} = 7.6 Hz, 0.9 Hz, 1H, C*H*), 7.05 (d, $^3J_{HH}$ = 7.9 Hz, 1H, C*H*), 7.14 (td, J_{HH} = 7.8, 1.3 Hz, 1H, C*H*), 7.98−7.99 (m, 1H, C*H*), 8.32−8.33 (m, 1H, C*H*). $^{13}C\{^1H\}$ NMR (176 MHz, CD_2Cl_2): δ 28.9 (d, J_{PC} = 4.3 Hz, P-C(CH_3)$_3$), 33.0 (d, J_{PC} = 30.6 Hz, Ar-CH_2-P), 35.7 (d, J_{PC} = 17.6 Hz, P-$C(CH_3)_3$), 107.8 (d, J_{PC} = 3.7 Hz), 110.7 (s), 122.9 (d, J_{PC} = 20.8 Hz), 126.4 (s), 126.6 (s), 139.8 (s), 142.6 (d, J_{PC} = 2.8 Hz), 143.5 (s), 150.7 (d, J_{PC} = 13.7 Hz). Anal. Calcd for $C_{19}H_{26}F_3N_2O_3PPdS$: C, 40.98; H, 4.71; N, 5.03. Found: C, 40.97; H, 4.56; N, 4.96.

[(PCN^H)Pd]$_2$(μ-OH)[OTf] (8a). Ground KOH (1.4 mg, 0.0250 mmol, 1 equiv) was added to a solution of **7a** (26.7 mg, 0.0479, 2 equiv) in THF (3 mL), and the mixture was stirred for 24 h. The golden mixture was filtered through Celite and concentrated (ca. 1 mL). The product was crystallized in a pentane-vapor diffusion chamber at −30 °C. The isolated golden crystals of **8a** were suitable for X-ray crystallography (16.0 mg, 68% yield). $^{31}P\{^1H\}$ NMR (202 MHz, THF-d_8): δ 93.3 (s). ^1H NMR (500 MHz, THF-d_8): δ −1.48 (s, 1H, Pd−O*H*), 1.44 (d, $^3J_{PH}$ = 14.1 Hz, 18H, P−C(CH_3)$_3$), 1.51 (d, $^3J_{PH}$ = 14.3 Hz, 18H, P−C(CH_3)$_3$), 3.54 (dd, $^2J_{PH}$ = 9.3 Hz, $^2J_{HH}$ = 18.1 Hz, 2H, Ar-CH_2-P), 3.58 (dd, $^2J_{PH}$ = 10.2 Hz, $^2J_{HH}$ = 18.1 Hz, 2H, Ar-CH_2-P), 6.40−6.42 (m, 2H, C*H*), 7.07 (dd, J_{HH} = 7.7, 1.1 Hz, 2H, C*H*), 7.11 (td, J_{HH} = 7.7, 1.3 Hz, 2H, C*H*), 7.34 (dd, J_{HH} = 7.8, 1.1 Hz, 2H, C*H*), 8.32−8.33 (m, 2H, C*H*), 8.45−8.46 (m, 2H, C*H*). $^{13}C\{^1H\}$ NMR (176 MHz, THF-d_8): δ 29.31 (d, J_{PC} = 4.4 Hz, P−C(CH_3)$_3$), 29.52 (d, J_{PC} = 4.4 Hz, P-C(CH_3)$_3$), 34.88 (d, J_{PC} = 31.3 Hz, Ar-CH_2-P), 35.86 (d, J_{PC} = 17.6 Hz, P-C(CH_3)$_3$), 36.13 (d, J_{PC} = 17.6 Hz, P-$C(CH_3)_3$), 107.56 (d, J_{PC} = 3.3 Hz), 111.48 (s), 123.34 (d, J_{PC} = 21.1 Hz), 126.62 (s), 128.11 (s), 140.41 (d, J_{PC} = 1.9 Hz), 144.59 (s), 144.65 (s), 151.13 (d, J_{PC} = 14.1 Hz). Anal. Calcd for $C_{37}H_{53}F_3N_4O_4P_2Pd_2S$: C, 45.27; H, 5.44; N, 5.71. Found: C, 46.17; H, 5.51; N, 5.49.

(PCN^H)Pd(OH) (9a) and (PCN^H)Pd(μ-OH)Pd(PCC) (10a). In a medium-walled NMR tube with a resealable Teflon pin, ground KOH (0.8 mg, 0.0143 mmol) was added to a solution of **7a** (7.0 mg, 0.0126

DOI: 10.1021/acs.organomet.5b00355
Organometallics XXXX, XXX, XXX−XXX

mmol) in THF-d_8 (0.4 mL). The mixture was shaken intermittently until full conversion to **8a** was observed by NMR spectroscopy. An excess of ground KOH (1.2 mg, 0.214 mmol) was then added, and the NMR tube was rotated slowly using a NMR tube rotary device over 16 h. Full conversion of **8a** to a mixture of **9a** (70% yield based on internal standard, hexamethylbenzene) and **10a** was observed by NMR spectroscopy. Compound **9a** can also be prepared by the addition of D_2O (0.1 mL) to a THF-d_8 (0.4 mL) solution of **8a** (5.0 mg, 8.98 μmol) containing suspended KOH (0.6 mg, 10.7 μmol). Using this procedure the resulting solution contained only **9a**, as determined by solution NMR spectroscopy.

Compound ***9a***. $^{31}P\{^1H\}$ NMR (202 MHz, THF-d_8): δ 91.9 (s). ^1H NMR (500 MHz, THF-d_8): δ −1.71 (s, 1H, Pd−O*H*), 1.43 (d, $^3J_{PH}$ = 13.9 Hz, 18H, P-C(CH_3)$_3$), 3.38 (d, $^2J_{PH}$ = 9.2 Hz, 2H, Ar-CH_2-P), 6.49 (m, 1H, C*H*), 6.92−6.95 (m, 2H, C*H*), 7.15 (m, 1H, C*H*), 8.05 (m, 1H, C*H*), 8.30 (m, 1H, C*H*). ^1H NMR (700 MHz, THF-d_8/D_2O): δ 1.38 (d, $^3J_{PH}$ = 14.1 Hz, 18H, P-C(CH_3)$_3$), 3.36 (d, $^2J_{PH}$ = 9.3 Hz, 2H, Ar-CH_2-P), 6.59−6.56 (m, 1H, C*H*), 6.93 (d, $^3J_{HH}$ = 7.5 Hz, 1H, C*H*), 6.98 (t, $^3J_{HH}$ = 7.6 Hz, 1H, C*H*), 7.18 (d, $^3J_{HH}$ = 7.8 Hz, 1H, C*H*), 8.08 (m, 1H, C*H*), 8.32 (m, 1H, C*H*). $^{13}C\{^1H\}$ NMR (176 MHz, THF-d_8/D_2O): δ 29.47 (d, J_{PC} = 4.8 Hz, P-C(CH_3)$_3$), 35.61 (d, J_{PC} = 31.0 Hz, Ar-CH_2-P), 35.75 (d, J_{PC} = 17.3 Hz, P-*C*(CH_3)$_3$), 107.98 (d, J_{PC} = 3.5 Hz), 110.61 (s), 122.57 (d, J_{PC} = 20.4 Hz), 125.72 (s), 127.21 (s), 140.72 (d, J_{PC} = 2.8 Hz), 144.8 (s), 147.85 (s), 150.96 (d, J_{PC} = 14.5 Hz). LRMS (ESI-MS) *m*/*z*: [M − OH]$^+$ calcd for $C_{18}H_{26}N_2PPd$ 407; found 407.3.

Compound ***10a***. $^{31}P\{^1H\}$ NMR (120 MHz, THF-d_8): δ 71.0 (s, *P trans* to C), 91.1 (s, *P trans* to N). ^1H NMR (700 MHz, THF-d_8): δ −1.75 (bs, 1H, Pd-O*H*), 1.36 (d, J = 12.4 Hz, 9H, P−C(CH_3)$_3$), 1.39 (d, J = 12.5 Hz, 9H, P−C(CH_3)$_3$), 1.44 (d, J = 13.8 Hz, 9H, P-C(CH_3)$_3$), 1.51 (d, J = 14.2 Hz, 9H, P-C(CH_3)$_3$), 3.08 (dd, $^2J_{PH}$ = 8.9 Hz, $^2J_{HH}$ = 17.4 Hz, 1H, Ar-CH_2-P), 3.12 (dd, $^2J_{PH}$ = 8.3 Hz, $^2J_{HH}$ = 17.4 Hz, 1H, Ar-CH_2-P), 3.42 (dd, $^2J_{PH}$ = 9.3 Hz, $^2J_{HH}$ = 17.9 Hz, 1H, Ar-CH_2-P), 3.49 (dd, $^2J_{PH}$ = 9.3 Hz, $^2J_{HH}$ = 17.9 Hz, 1H, Ar-CH_2-P), 6.11−6.12 (m, 1H, C*H*), 6.31−6.32 (m, 1H, C*H*), 6.60 (d, J = 7.6 Hz, 1H, C*H*), 6.74 (td, J = 7.6, 1.1 Hz, 1H, C*H*), 6.90−6.91 (m, 1H, C*H*), 6.91−6.93 (m, 1H, C*H*), 6.96−6.98 (m, 1H, C*H*), 7.02 (td, J = 7.7, 1.0 Hz, 1H, C*H*), 7.16−7.18 (m, 1H, C*H*), 8.17−8.19 (m, 1H, C*H*), 8.74−8.75 (m, 1H, C*H*).

(PCN^{Me})Pd(OTf) (7b). AgOTf (42.1 mg, 0.164 mmol) was added to a solution of (PCN^{Me})PdCl (75.0 mg, 0.164 mmol) in CH_2Cl_2 (3 mL) in the absence of light. The suspension was stirred for 5 h and filtered through Celite. Layering pentane on the CH_2Cl_2 solution at room temperature gave clear light yellow crystals of **7b** suitable for X-ray crystallography (81.8 mg, 87% yield). $^{31}P\{^1H\}$ NMR (202 MHz, CD_2Cl_2): δ 92.1 ppm (s). ^1H NMR (500 MHz, CD_2Cl_2): δ 1.42 (d, $^3J_{PH}$ = 14.5 Hz, 18H, P-C(CH_3)$_3$), 2.68 (s, 3H, pyz-CH_3), 3.29 (d, $^2J_{PH}$ = 9.59 Hz, 2H, Ar-CH_2-P), 6.28 (s, 1H, C*H*), 7.01 (d, $^3J_{HH}$ = 7.11 Hz, 1H, C*H*), 7.13 (t, $^3J_{HH}$ = 7.11 Hz, 1H, C*H*), 7.19 (d, $^3J_{HH}$ = 7.51 Hz, 1H, C*H*), 8.22 (s, 1H, C*H*). $^{13}C\{^1H\}$ NMR (126 MHz, CD_2Cl_2): δ 14.56 (s, pyz-CH_3), 28.96 (d, $^2J_{PC}$ = 3.9 Hz, P(C(CH_3)$_3$)$_2$), 32.96 (d, $^1J_{PC}$ = 29.8 Hz, P(C(CH_3)$_3$)$_2$), 35.49 (d, $^1J_{PC}$ = 17.3 Hz, CH_2P), 109.3 (d, J_{PC} = 2.75 Hz), 112.3 (s), 122.5 (d, J_{PC} = 20.8 Hz), 126.4 (s), 140.6 (d, J_{PC} = 2.1 Hz), 140.9 (s), 141.9 (s), 145.2 (s), 150.9 (d, J_{PC} = 13.8 Hz). Anal. Calcd for $C_{20}H_{28}F_3N_2O_3PPdS$: C, 42.08; H, 4.94; N, 4.91. Found: C, 42.06; H, 4.81; N, 4.75.

[(PCN^{Me})Pd]$_2$(μ-OH)[OTf] (8b). To a solution of (PCN^{Me})Pd-(OTf) (14.5 mg, 0.0254 mmol) in THF (3 mL) was added ground KOH (1.0 mg, 0.0178 mmol). The solution was stirred for 16 h, after which it was filtered through a Teflon filter. The solution was concentrated (ca. 1 mL), and recrystallization was accomplished by slow diffusion of pentane into the solution at −30 °C. The dark yellow crystals were washed with water (3 × 1 mL) and dried under vacuum, giving **8b** (11.8 mg, 92% yield). $^{31}P\{^1H\}$ NMR (202 MHz, THF-d_8): δ 91.6 ppm (s). ^1H NMR (700 MHz, THF-d_8): δ −1.46 (s, 1H, Pd-O*H*), 1.43 (d, $^3J_{PH}$ = 14.0 Hz, 18H, P-C(CH_3)$_3$), 1.49 (d, $^3J_{PH}$ = 14.2 Hz, 18H, P-C(CH_3)$_3$), 2.67 (s, 3H, CH_3), 3.54 (dd, $^2J_{HH}$ = 18.1, $^2J_{PH}$ = 10.1 Hz, 2H, Ar-CH_2-P), 3.58 (dd, $^2J_{HH}$ = 18.1, $^2J_{PH}$ = 10.0 Hz, 2H, Ar-CH_2-P), 6.20 (m, 2H, C*H*), 7.10 (dd, $^3J_{HH}$ = 7.7 Hz, 1.4 Hz, 2H, C*H*), 7.12 (td, $^3J_{HH}$ = 7.6, 1.1 Hz, 2H, C*H*), 7.30 (dd, $^3J_{HH}$ = 7.7, 1.4 Hz, 2H, C*H*), 8.34 (m, 2H, C*H*). $^{13}C\{^1H\}$ NMR (176 MHz, THF-d_8): δ 14.1 (s, pyz-CH_3), 29.30 (d, J = 4.0 Hz, P(C(CH_3)$_3$)$_2$), 29.58 (d, J = 4.0 Hz, P(C(CH_3)$_3$)$_2$), 34.82 (d, J = 30.6 Hz, CH_2P), 35.65 (d, J = 17.6 Hz, P(C(CH_3)$_3$)$_2$), 36.00 (d, J = 17.7 Hz, P(*C*(CH_3)$_3$)$_2$), 108.9 (d, J = 1.6 Hz, pyz-*C*), 112.8 (s, Ar-*C*), 123.14 (d, J = 20.9 Hz, Ar-*C*), 126.4 (s, pyz-*C*), 139.7 (s, pyz-*C*), 141.8 (s, Ar-*C*), 145.7 (s, Ar-*C*), 145.8 (s, Ar-*C*), 151.48 (d, J = 14.2 Hz, Ar-*C*). Anal. Calcd for $C_{39}H_{57}F_3N_4O_4P_2Pd_2S$: C, 46.39; H, 5.69; N, 5.55. Found: C, 47.02; H, 5.70; N, 5.26.

(PCN^{Me})Pd(OH) (9b). To a solution of **4a** (30.0 mg, 0.0656 mmol) in THF (5 mL) was added an excess of ground KOH (15.2 mg, 0.271 mmol). The mixture was sonicated for 2.5 h and then left for 20 h at room temperature. The mixture was filtered through Celite and concentrated to ca. 1 mL. The golden solution was layered with pentane and cooled to −30 °C to yield tan crystals of **9b** suitable for X-ray diffraction (20.3 mg, 71% yield). $^{31}P\{^1H\}$ NMR (121 MHz, THF-d_8): δ 90.2 ppm (s). ^1H NMR (500 MHz, THF-d_8): δ −1.97 (s, 1H, Pd-O*H*), 1.43 (d, $^3J_{PH}$ = 13.7 Hz, 18H, P-C(CH_3)$_3$), 2.66 (s, 3H, CH_3), 3.36 (d, $^2J_{PH}$ = 9.2 Hz, 2H, Ar-CH_2-P), 6.25 (m, 1H, C*H*), 6.91−6.93 (m, 2H, C*H*), 7.17 (dd, $^3J_{HH}$ = 6.1, 2.8 Hz, 1H, C*H*), 7.79 (m, 1H, C*H*). $^{13}C\{^1H\}$ NMR (126 MHz, THF-d_8): δ 14.07 (s, pyz-CH_3), 29.40 (d, J = 5.0 Hz, P(C(CH_3)$_3$)$_2$), 35.38 (d, J = 16.9 Hz), 36.16 (d, J = 28.9 Hz), 108.1 (s), 111.6 (s), 121.89 (d, J = 20.2 Hz), 124.1 (s), 138.1 (s), 140.2 (s), 146.3 (s), 150.90 (d, J = 14.8 Hz). Anal. Calcd for $C_{19}H_{29}N_2OPPd$: C, 52.00; H, 6.66; N, 6.38. Found: C, 51.89; H, 6.76; N, 6.18.

■ ASSOCIATED CONTENT

Ⓢ Supporting Information

Tables, figures, and CIF and XYZ files giving selected crystallographic parameters of the solved XRD structures, NMR spectra of all the described compounds, and Cartesian coordinates and absolute G_{THF} energy values of the optimized structures of **9a**, **9a′**, **TS$_{rot}$**, **TS$_1$**, **10a**···H_2O, and **11a**. The Supporting Information is available free of charge on the ACS Publications website at DOI: 10.1021/acs.organomet.5b00355.

■ AUTHOR INFORMATION

Corresponding Authors

*E-mail for R.A.K.: rakemp@unm.edu.

*E-mail for G.G.: giuliano.giambastiani@iccom.cnr.it.

*E-mail for K.I.G.: goldberg@chem.washington.edu.

Notes

The authors declare no competing financial interest.

■ ACKNOWLEDGMENTS

L.L., A.R., and G.G. thank the Fondazione Cariplo ("Crystalline Elastomers" project), the *Groupe de Recherche International* (GDRI) "*Homogeneous Catalysis for Sustainable Development*", and the COST action CM1006: "EUFEN: European F-Element Network" for supporting this work. CREA (Centro Ricerche Energia e Ambiente) in Colle Val d'Elsa (Siena, Italy) is also acknowledged for computational resources. The work done at the University of Washington and the University of New Mexico was supported by the Department of Energy (DE-FG02-06ER15765).

■ REFERENCES

(1) For general reviews and books, see: (a) *Pincer and Pincer-Type Complexes: Application in Organic Synthesis and Catalysis*; Szabo, K. J., Wendt, O. F., Eds.; Wiley-VCH: Weinheim, Germany, 2014. (b) *Organometallic Pincer Chemistry*; van Koten, G., Milstein, D., Eds.; Springer: Heidelberg, Germany, 2013; Top. Organomet. Chem. *40*. (c) Niu, J.-L.; Hao, X.-Q.; Gong, J.-F.; Song, M.-P. *Dalton Trans* **2011**, *40*, 5135−5150. (d) Benito-Garagorri, D.; Kirchner, K. *Acc. Chem. Res.*

DOI: 10.1021/acs.organomet.5b00355
Organometallics XXXX, XXX, XXX−XXX

2008, *41*, 201−213. (e) van der Boom, M. E.; Milstein, D. *Chem. Rev.* **2003**, *103*, 1759−1792. (f) Singleton, J. T. *Tetrahedron* **2003**, *59*, 1837−1857.

(2) Roesky, H. W.; Singh, S.; Yusuff, K. K. M.; Maguire, J. A.; Hosmane, N. S. *Chem. Rev.* **2006**, *106*, 3813−3843.

(3) Wenzel, T. T. *Stud. Surf. Sci. Catal.* **1991**, *66*, 545−554.

(4) Bailey, W. D.; Parkes, M. V.; Kemp, R. A.; Goldberg, K. I. Reactions of Square Planar d^8 Pincer Complexes with Oxygen and Hydrogen. In *Pincer and Pincer-Type Complexes: Application in Organic Synthesis and Catalysis*; Szabo, K. J., Wendt, O. F., Eds.; Wiley-VCH: Weinheim, Germany, 2014; pp 281−298.

(5) The pioneering work on PCP-pincer complexes is: (a) Moulton, C. J.; Shaw, B. L. *J. Chem. Soc., Dalton Trans.* **1976**, 1020−1024. More recent (selected) examples are as follows. PCP type: (b) Roddick, D. M. *Top. Organomet. Chem.* **2013**, *40*, 49−88. (c) Kundu, S.; Choliy, Y.; Zhuo, G.; Ahuja, R.; Emge, T. J.; Warmuth, R.; Brookhart, M.; Krogh-Jespersen, K.; Goldman, A. S. *Organometallics* **2009**, *28*, 5432−5444. (d) Leis, W.; Mayer, H. A.; Kaska, W. C. *Coord. Chem. Rev.* **2008**, *252*, 1787−1797. (e) Jensen, C. M. *Chem. Commun.* **1999**, 2443−2449. PNP type: (f) Schneider, S.; Meiners, J.; Askevold, B. *Eur. J. Inorg. Chem.* **2012**, *2012*, 412−429. (g) Milstein, D. *Top. Catal.* **2010**, *53*, 915−923. POCOP type: (h) Timpa, S. D.; Pell, C.; Zhou, J.; Ozerov, O. V. *Organometallics* **2014**, *33*, 5254−5262. (i) Jonasson, K. J.; Wendt, O. F. *Chem. - Eur. J.* **2014**, *20*, 11894−11902. (j) Lao, D. B.; Owens, A. C. E.; Heinekey, D. M.; Goldberg, K. I. *ACS Catal.* **2013**, *3*, 2391−2396. (k) Pandarus, V.; Zargarian, D. *Chem. Commun.* **2007**, 978−980. (l) Hebden, T. J.; St. John, A. J.; Gusev, D. G.; Kaminsky, W.; Goldberg, K. I.; Heinekey, D. M. *Angew. Chem., Int. Ed.* **2011**, *50*, 1873−1876.

(6) Some (selected) examples are as follows. CCN/CNN/NCN′ type: (a) Luconi, L.; Klosin, J.; Smith, A. J.; Germain, S.; Schulz, E.; Hannedouche, J.; Giambastiani, G. *Dalton Trans.* **2013**, *42*, 16056−16065. (b) Luconi, L.; Rossin, A.; Motta, A.; Tuci, G.; Giambastiani, G. *Chem. - Eur. J.* **2013**, *19*, 4906−4921. (c) Bröring, M.; Kleeberg, C.; Köhler, S. *Inorg. Chem.* **2008**, *47*, 6404−6412. PNN type: (d) Balaraman, E.; Gunanathan, C.; Zhang, J.; Shimon, L. J. W.; Milstein, D. *Nat. Chem.* **2011**, *3*, 609−614. (e) Gnanaprakasam, B.; Milstein, D. *J. Am. Chem. Soc.* **2011**, *133*, 1682−1685. (f) Zhang, J.; Balaraman, E.; Leitus, G.; Milstein, D. *Organometallics* **2011**, *30*, 5716−5724. (g) Balaraman, E.; Gnanaprakasam, B.; Shimon, L. J. W.; Milstein, D. *J. Am. Chem. Soc.* **2010**, *132*, 16756−16758. PCO type: (h) Fulmer, G. R.; Kaminsky, W.; Kemp, R. A.; Goldberg, K. I. *Organometallics* **2011**, *30*, 1627−1636. PCS type: (i) Li, J.; Siegler, M.; Lutz, M.; Spek, A. L.; Gebbink, R. J. M. K.; van Koten, G. *Adv. Synth. Catal.* **2010**, *352*, 2474−2488. (j) Gagliardo, M.; Selander, N.; Mehendale, N. C.; van Koten, G.; Klein G, R. J. M.; Szabó, K. J. *Chem. - Eur. J.* **2008**, *14*, 4800−4809.

(7) Examples of PCN type complexes can be found in: (a) Hao, X.-Q.; Huang, J.-J.; Wang, T.; Lv, J.; Gong, J.-F.; Song, M.-P. *J. Org. Chem.* **2014**, *79*, 9512−9530. (b) Khake, S. M.; Soni, V.; Gonnade, R. G.; Punji, B. *Dalton Trans.* **2014**, *43*, 16084−16096. (c) Herbert, D. E.; Ozerov, O. V. *Organometallics* **2011**, *30*, 6641−6654. (d) Moreno, I.; SanMartin, R.; Inés, B.; Herrero, M. T.; Domínguez, E. *Curr. Org. Chem.* **2009**, *13*, 878−895. (e) Poverenov, E.; Leitus, G.; Shimon, L. J. W.; Milstein, D. *Organometallics* **2005**, *24*, 5937−5944.

(8) Mehendale, N. C.; Sietsma, J. R. A.; de Jong, K. P.; van Walree, C. A.; Klein Gebbink, R. J. M.; van Koten, G. *Adv. Synth. Catal.* **2007**, *349*, 2619−2630.

(9) As a comparison of the catalytic activities of NCP and NCN pyrazole-based pincers, see: (a) Zhang, X.; Suzuki, S.; Kozaki, M.; Okada, K. *J. Am. Chem. Soc.* **2012**, *134*, 17866−17868. (b) Inés, B.; SanMartin, R.; Churruca, F.; Domínguez, E.; Urtiaga, M. K.; Arriortua, M. I. *Organometallics* **2008**, *27*, 2833−2839. (c) Gong, J.-F.; Zhang, Y.-H.; Song, M.-P.; Xu, C. *Organometallics* **2007**, *26*, 6487−6492.

(10) (a) Chierotti, M. R.; Rossin, A.; Gobetto, R.; Peruzzini, M. *Inorg. Chem.* **2013**, *52*, 12616−12623. (b) Rossin, A.; Bottari, G.; Lozano-Vila, A. M.; Paneque, M.; Peruzzini, M.; Rossi, A.; Zanobini, F. *Dalton Trans.* **2013**, *42*, 3533−3541. (bb) Levina, V. A.; Rossin, A.; Belkova, N. V.; Chierotti, M. R.; Epstein, L. M.; Filippov, O. A.; Gobetto, R.; Gonsalvi, L.; Lledòs, A.; Shubina, E. S.; Zanobini, F.; Peruzzini, M. *Angew. Chem., Int. Ed.* **2011**, *50*, 1367−1370. (c) Rossin, A.; Peruzzini, M.; Zanobini, F. *Dalton Trans.* **2011**, *40*, 4447−4452. (d) Fulmer, G. R.; Herndon, A. N.; Kaminsky, W.; Kemp, R. A.; Goldberg, K. I. *J. Am. Chem. Soc.* **2011**, *133*, 17713−17726. (e) Denney, M. C.; Smythe, N. A.; Cetto, K. L.; Kemp, R. A.; Goldberg, K. I. *J. Am. Chem. Soc.* **2006**, *128*, 2508−2509.

(11) Bailey, W. D.; Kaminsky, W.; Kemp, R. A.; Goldberg, K. I. *Organometallics* **2014**, *33*, 2503−2509.

(12) (a) Luconi, L.; Rossin, A.; Tuci, G.; Germain, S.; Schulz, E.; Hannedouche, J.; Giambastiani, G. *ChemCatChem* **2013**, *5*, 1142−1151. (b) Luconi, L.; Rossin, A.; Tuci, G.; Tritto, I.; Boggioni, L.; Klosin, J. J.; Theriault, C. N.; Giambastiani, G. *Chem. - Eur. J.* **2012**, *18*, 671−687. (c) Luconi, L.; Giambastiani, G.; Rossin, A.; Bianchini, C.; Lledós, A. *Inorg. Chem.* **2010**, *49*, 6811−6813. (d) Luconi, L.; Lyubov, D. M.; Bianchini, C.; Rossin, A.; Faggi, C.; Fukin, G. K.; Cherkasov, A. V.; Shavyrin, A. S.; Trifonov, A. A.; Giambastiani, G. *Eur. J. Inorg. Chem.* **2010**, *2010*, 608−620. (e) Lyubov, D. M.; Fukin, G. K.; Cherkasov, A. V.; Shavyrin, A. S.; Trifonov, A. A.; Luconi, L.; Bianchini, C.; Meli, A.; Giambastiani, G. *Organometallics* **2009**, *28*, 1227−1232.

(13) Yang, L.; Powell, D. R.; Houser, R. P. *Dalton Trans.* **2007**, 955−964.

(14) The (few) structurally determined (PCN)PdCl complexes can be found in: (a) Cook, E.; Iwasaki, K.; Masuda, J. D.; Xia, A. *Polyhedron* **2015**, *87*, 38−42. (b) Hou, A.-T.; Liu, Y.-L.; Hao, X.-Q.; Gong, J.-F.; Song, M.-P. *J. Organomet. Chem.* **2011**, *696*, 2857−2862. (c) Gong, J.-F.; Zhang, Y.-H.; Song, M.-P.; Xu, C. *Organometallics* **2007**, *26*, 6487−6492. (d) Motoyama, Y.; Shimozono, K.; Nishiyama, H. *Inorg. Chim. Acta* **2006**, *359*, 1725−1730.

(15) Some examples are as follows. (a) (^{tBu}PCP)PdCl: Johnson, M. T.; Dzolic, Z.; Cetina, M.; Lahtinen, M.; Ahlquist, M. S. G.; Rissanen, K.; Ohrstrom, L.; Wendt, O. F. *Dalton Trans.* **2013**, *42*, 8484−8491. (b) (^{tBu}PCP)Pd(COOH): Johansson, R.; Wendt, O. F. *Organometallics* **2007**, *26*, 2426−2430. (c) (^{tBu}PCP)Pd(I_3): Johnson, M. T.; Dzolic, Z.; Cetina, M.; Wendt, O. F.; Ohrstrom, L.; Rissanen, K. *Cryst. Growth Des.* **2012**, *12*, 362−368.

(16) (a) Hartshorn, C. M.; Steel, P. J. *Organometallics* **1998**, *17*, 3487−3496. (b) Canty, A. J.; Patel, J.; Skelton, B. W.; White, A. H. *J. Organomet. Chem.* **2000**, *607*, 194−202.

(17) Surprisingly, there are very few examples of crystallographically characterized palladium dimers bridged by only one chlorine atom: (a) Grove, D. M.; van Koten, G.; Ubbels, H. J. C.; Spek, A. L. *J. Am. Chem. Soc.* **1982**, *104*, 4285−4286. (b) Fornies, J.; Navarro, R.; Sicilia, V.; Martinez, F.; Welch, A. J. *J. Organomet. Chem.* **1991**, *408*, 425−437. (c) Ara, I.; Fornies, J.; Martin, A.; Martin, L. F.; Menjon, B.; Miedes, H. *Dalton Trans.* **2010**, *39*, 7301−7309.

(18) Bryndza, H. E.; Tam, W. *Chem. Rev.* **1988**, *88*, 1163−1188.

(19) Cámpora, J.; Palma, P.; del Río, D.; Álvarez, E. *Organometallics* **2004**, *23*, 1652−1655.

(20) Some examples are: (a) Khusnutdinova, J. R.; Rath, N. P.; Mirica, L. M. *J. Am. Chem. Soc.* **2012**, *134*, 2414−2422. (b) Cao, L.; Jennings, M. C.; Puddephatt, R. J. *Dalton Trans.* **2009**, 5171−5176. (c) Klein, A.; Dogan, A.; Feth, M.; Bertagnolli, H. *Inorg. Chim. Acta* **2003**, *343*, 189−201.

(21) Joslin, E. E.; Quillian, B.; Gunnoe, T. B.; Cundari, T. R.; Sabat, M.; Myers, W. H. *Inorg. Chem.* **2014**, *53*, 6270−6279.

(22) (a) Salanouve, E.; Retailleau, P.; Janin, Y. L. *Tetrahedron* **2012**, *68*, 2135. (b) Alonso, M. T.; Juanes, O.; de Mendoza, J.; Rodríguez-Ubis, J. C. *J. Organomet. Chem.* **1994**, *484*, 19−26.

(23) (a) Canty, A. J.; Honeyman, R. T.; Skelton, B. W.; White, A. H. *Inorg. Chim. Acta* **1986**, *114*, L39−L42. (b) Canty, A. J.; Minchin, N. J. *J. Organomet. Chem.* **1982**, *226*, C14−C16. (c) Canty, A. J.; Honeyman, R. T. *J. Organomet. Chem.* **1992**, *430*, 245−257. (d) Canty, A. J.; Honeyman, R. T. *J. Organomet. Chem.* **1990**, *387*, 247−263.

(24) (a) Maenaka, Y.; Suenobu, T.; Fukuzumi, S. *J. Am. Chem. Soc.* **2012**, *134*, 9417−9427. (b) Wiley, J. S.; Oldham, W. J., Jr.; Heinekey, D. M. *Organometallics* **2000**, *19*, 1670−1676.

DOI: 10.1021/acs.organomet.5b00355
Organometallics XXXX, XXX, XXX−XXX

(25) Petit, A.; Flygare, J.; Miller, A. T.; Winkel, G.; Ess, D. H. *Org. Lett.* **2012**, *14*, 3680−3683.
(26) (a) Johansson, R.; Öhrström, L.; Wendt, O. F. *Cryst. Growth Des.* **2007**, *7*, 1974−1979.
(27) (a) Hayashi, Y.; Wada, S.; Yamashita, M.; Nozaki, K. *Organometallics* **2012**, *31*, 1073−1081. (b) Canty, A. J.; Jin, H.; Roberts, A. S.; Skelton, B. W.; White, A. H. *Organometallics* **1996**, *15*, 5713−5722. (c) Canty, A. J.; Jin, H.; Skelton, B. W.; White, A. H. *J. Organomet. Chem.* **1995**, *503*, C16. (d) Castan, P.; Dahan, F.; Wimmer, S.; Wimmer, F. L. *J. Chem. Soc., Dalton Trans.* **1990**, 2679−2683.
(28) Fulmer, G. R.; Muller, R. P.; Kemp, R. A.; Goldberg, K. I. *J. Am. Chem. Soc.* **2009**, *131*, 1346−1347.
(29) *APEX2 (Version 2.1-4), SAINT (version 7.34A), and SADABS (version 2007/4)*; BrukerAXS Inc., Madison, WI, USA, 2007.
(30) *CrysAlis CCD 1.171.31.2 (release 07-07-2006), CrysAlis171.NET*, Oxford Diffraction Ltd.
(31) *CrysAlis RED 1.171.31.2 (release 07-07-2006), CrysAlis171.NET*, Oxford Diffraction Ltd.
(32) Altomare, A.; Burla, M. C.; Camalli, M.; Cascarano, G. L.; Giacovazzo, C.; Guagliardi, A.; Moliterni, A. G. G.; Polidori, G.; Spagna, R. *J. Appl. Crystallogr.* **1999**, *32*, 115−119.
(33) Sheldrick, G. M. *SHELXL*; University of Göttingen, Göttingen, Germany, 1997.
(34) Nardelli, M. *Comput. Chem.* **1983**, *7*, 95−98.
(35) Farrugia, L. J. *J. Appl. Crystallogr.* **1997**, *30*, 565.
(36) Frisch, M. J. et al.. *Gaussian09, Revision C.01*; Gaussian Inc., Wallingford, CT, 2009.
(37) Zhao, Y.; Truhlar, D. G. *Theor. Chem. Acc.* **2008**, *120*, 215−241.
(38) (a) Andrae, D.; Haeuessermann, U.; Dolg, M.; Stoll, H.; Preuss, H. *Theor. Chem. Acc.* **1990**, *77*, 123−141. (b) Dunning Jr., T. H.; Hay, P. J. In *Modern Theoretical Chemistry*; Schaefer, H. F., III, Ed.; Plenum: New York, 1976; Vol. 3, pp 1−28.
(39) Lynch, B. J.; Zhao, Y.; Truhlar, D. G. *J. Phys. Chem. A* **2003**, *107*, 1384−1388.
(40) (a) Höllwarth, A.; Böhme, M.; Dapprich, S.; Ehlers, A. W.; Gobbi, A.; Jonas, V.; Köhler, K. F.; Stegmann, R.; Veldkamp, A.; Frenking, G. *Chem. Phys. Lett.* **1993**, *208*, 237−240. (b) Ehlers, A. W.; Böhme, M.; Dapprich, S.; Gobbi, A.; Höllwarth, A.; Jonas, V.; Köhler, K. F.; Stegmann, R.; Veldkamp, A.; Frenking, G. *Chem. Phys. Lett.* **1993**, *208*, 111−114.
(41) Fukui, K. *Acc. Chem. Res.* **1981**, *14*, 363−368.
(42) Marenich, A. V.; Cramer, C. J.; Truhlar, D. G. *J. Phys. Chem. B* **2009**, *113*, 6378−6396.

DOI: 10.1021/acs.organomet.5b00355
Organometallics XXXX, XXX, XXX−XXX